

NATIONAL ADVISORY COMMITTEE FOR AERONAUTICS

TECHNICAL NOTE 2690

CONDENSATION OF AIR IN SUPERSONIC WIND TUNNELS AND ITS EFFECTS ON FLOW ABOUT MODELS

By C. Frederick Hansen and George J. Nothwang

Ames Aeronautical Laboratory
Moffett Field, Calif.

PROPERTY FAIRCHILD
ENGINEERING LIBRARY



Washington

April 1952

NATIONAL ADVISORY COMMITTEE FOR AERONAUTICS

TECHNICAL NOTE 2690

CONDENSATION OF AIR IN SUPERSONIC WIND TUNNELS

AND ITS EFFECTS ON FLOW ABOUT MODELS

By C. Frederick Hansen and George J. Nothwang

SUMMARY

Results of an investigation of condensation phenomena in supersonic wind tunnels are presented. Lower and upper limits for the degree of supersaturation attainable before the onset of condensation of air are discussed. The upper limit is derived from the Becker-Döring theory of self-nucleation using a surface tension corrected for droplet size. The lower limit is calculated from the saturation vapor pressure of air. Experimental data obtained in the Ames 10- by 14-inch supersonic wind tunnel and a 1- by 1.4-inch supersonic nozzle indicate that silica gel particles or small amounts of water vapor in an air stream will initiate condensation near the lower limit. Tests with the 1- by 1.4-inch supersonic nozzle indicate that dry air and nitrogen may achieve considerable supersaturation before condensation occurs. However, relatively elaborate means of air purification are required to attain this supersaturation; thus, increasing the stagnation temperature so that the expanded stream flow is subsaturated still appears to be the most practical means of obtaining substantial increase in the Mach number of condensation-free flow in wind tunnels.

A method is presented for calculating the properties of a stream containing a small fraction of condensed air. By use of this method, it is found that evaporation of condensed phase may change the stream properties appreciably in the compression flow regions about models. Pressures measured on the surface of a 10° wedge substantiate these findings.

Scattering of light from droplets of condensed phase is exploited to demonstrate the extent of condensation in supersonic air streams and in the flow about models.

INTRODUCTION

Condensation phenomena were encountered early in supersonic research when the usual mixtures of water vapor and air taken from the atmosphere

were expanded beyond the water-vapor saturation conditions in supersonic wind tunnels. Condensation of the vapor-phase water was found to result in undesirable condensation shocks (see, e.g., reference 1), but these could be eliminated by drying the air supply.

In extending the range of supersonic research to higher Mach numbers, the problem of condensation in wind tunnels is re-encountered, since saturation conditions of the air itself may be reached or exceeded. Bogdonoff and Lees (reference 2) investigated this problem and, finding no shock discontinuity in flow with conditions theoretically exceeding saturation, concluded that condensation of air did not occur. Later, Becker (reference 3) presented evidence from the Langley 11-inch hypersonic wind tunnel that condensation of air may occur as a gradual process without causing a shock and that the process is initiated when static stream properties are near saturation conditions. Wegener, Stollenwerk, Reed, and Lundquist (reference 4) and Buhler (reference 5) have reported similar results, although somewhat different degrees of supersaturation were apparently attained.

One obvious way to circumvent the problems associated with condensation of air in supersonic wind tunnels is to prevent the occurrence of condensation by using elevated reservoir temperatures so that saturation conditions are not reached in the expanded flow. This method has been used successfully by numerous investigators and typical results are reported in references 3 and 4. However, as the Mach number is increased, the reservoir temperatures required to maintain subsaturated flow conditions become extremely high and ultimately impractical; therefore, it is important to know whether condensation of air may be prevented by methods other than heating the reservoir supply air. Since it may not be practical to prevent condensation in all cases, another important question is whether useful experimental data can be abstracted from tests conducted in a supersonic air stream with condensed phase. Accordingly, a theoretical and experimental investigation was undertaken at the Ames Laboratory to determine whether the Mach number range of condensation-free flow may be extended by achieving a relatively stable supersaturated state and, further, if the effects of condensation on flow about models may be quantitatively evaluated. The results of this investigation are the subject of the present report.

SYMBOLS

α angle of attack, degrees

H total pressure, atmospheres

i specific enthalpy, calories per gram

J nucleation frequency, nuclei per cubic centimeter per second

k Boltzmann constant, ergs per degree Kelvin

log logarithm to base 10

M Mach number

M_A Mach number from nozzle-area ratio

M_H pitot Mach number (determined from the ratio of pitot to reservoir pressure $\frac{H_5}{H_0}$ assuming adiabatic flow)

M_p static Mach number (determined from the ratio of static to reservoir pressure $\frac{P_2}{H_0}$ assuming isentropic flow)

M_{pH} pitot-static Mach number (determined from the ratio of static to pitot pressure $\frac{P_2}{H_5}$ and Rayleigh's formula)

~~free stream conditions before condensation~~

p static pressure, millimeters of mercury

p_∞ saturation vapor pressure of air, millimeters of mercury

Q heat added or subtracted from air stream, calories per gram

T temperature, degrees Kelvin

u ratio of stream velocity to velocity of sound referred to conditions where $M = 1$

V stream velocity, centimeters per second

γ ratio of specific heat at constant pressure to specific heat at constant volume

ρ density of vapor phase air, grams per cubic centimeter

Subscripts

o reservoir conditions

1 free-stream conditions before condensation

2 free-stream conditions with condensation

- 3 conditions just downstream of a shock wave assuming no evaporation of condensed air
- 4 conditions downstream of a shock wave assuming evaporation of condensed air to equilibrium condition
- 5 equilibrium stagnation conditions downstream of a normal shock wave

Superscripts

- * threshold conditions (conditions at which condensation is initiated)

THEORETICAL CONSIDERATIONS

This investigation is first of all concerned with the mechanism of condensation, particularly insofar as it dictates the threshold conditions (conditions at the onset of condensation). In addition, it will be undertaken to determine some effects of condensation on the stream properties and on the forces experienced by models in supersonic flow.

Mechanism of Condensation

It is convenient to study the mechanism of air condensation first assuming that air is a mixture of pure oxygen and nitrogen, and then separately considering the effects of impurities in the mixture. Some supersaturation of a pure vapor is usually possible, and there is no obvious reason to expect a pure oxygen and nitrogen mixture to behave differently. However, the supersaturated state must ultimately collapse when aggregates of vapor molecules grow large enough to serve as nuclei on which condensation to liquid or solid¹ phase can proceed. A kinetic theory of this self-nucleation process has been developed by Becker and Döring (reference 6). In deriving their expression for nucleation frequency, Becker and Döring assumed that the surface tension of liquid

¹Sublimation as well as liquefaction may occur at the low static temperatures and pressures attainable in wind-tunnel flow. It is assumed that theories of liquefaction may be extended slightly beyond the triple point, without serious error, by using sublimation vapor pressures in place of the liquefaction vapor pressures.

droplets was independent of droplet size and equal to that for a plane liquid surface. It is now known that surface tension decreases with decreasing droplet size and this effect has been calculated by Tolman (reference 7) and more recently by Stever and Rathbun (reference 8), among others. The surface tension does not change order of magnitude, however. Consequently, it may easily be demonstrated that the expression obtained by Becker and Döring for nucleation frequency remains valid if the value of surface tension for a critical size droplet (defined as a droplet in equilibrium with the vapor) is used in place of the surface tension for bulk liquid. Using Tolman's correction to surface tension, because of its relatively simple form, the nucleus formation rates were calculated from the Becker-Döring theory (appendix A). The results of such a calculation are shown in figure 1 for various reservoir temperatures and a reservoir pressure of 6 atmospheres.

This nucleation theory does not specify what nucleation frequency shall be the criterion for the onset of condensation. Durbin (reference 9) found that measurements of light scattering from droplets of condensed phase indicated concentrations of about 10^{10} particles per cubic centimeter in a partially condensed air stream in the Langley 11-inch hypersonic tunnel. This particle concentration would require nucleation rates of the order of 10^{12} nuclei per cubic centimeter per second. The nucleation rate at threshold conditions would, of course, be somewhat less. The precise value chosen as the criterion for threshold is not critical, however, since the nucleus formation rate is a steep function of Mach number (see fig. 1). Accordingly, 10^{12} nuclei per cubic centimeter per second is chosen for this criterion.

In reality, of course, air is not a mixture of pure oxygen and nitrogen, but contains water vapor, carbon dioxide, and other impurities which conceivably may serve as nuclei and initiate condensation at less supersaturation than required for self-nucleation. Consequently, the Becker-Döring analysis should only be expected to yield a limiting threshold supersaturation. The corresponding Mach number will be designated as the theoretical maximum threshold Mach number.

Concerning the behavior of impurities in a supersaturated vapor, Frenkel (reference 10) points out that such impurities are not automatically condensation nuclei by virtue of possessing a size greater than the critical size droplet required for self-nucleation. Rather, the direction of change in free energy, as surface films of vapor molecules form on the embryos, determines whether or not condensation on such embryos is thermodynamically possible. Since the free-energy function depends on the composition of the vapor and of the embryo impurities, it is expected that in a given vapor each type of impurity may exhibit a different characteristic threshold of condensation. Indeed, Schaefer (reference 11) found this to be the case for the nucleation of ice crystals.

An additional factor which should be considered in estimating the potential of vapor impurities to initiate condensation in wind tunnels

is the time interval of flow to the test section during which the vapor impurity is supersaturated, since some time is required to develop aggregates of the impurity with sufficient size to function as condensation nuclei for air. In appendix B the embryo sizes attained by carbon dioxide and water vapor in typical wind-tunnel flow are estimated to be the same order of magnitude as the critical size required for self-nucleation. Reasoning qualitatively, Frenkel (reference 10) shows that a foreign nucleus must generally be larger than this critical size. Thus, while both carbon dioxide and water vapor may be sources of nuclei, the decrease in embryo growth rate attending a reduction in concentration of these impurities may significantly reduce their potential for initiating condensation in wind-tunnel flow. It will be useful to refer to this conclusion when interpreting experimental data to be discussed subsequently.

In general, the form of the surface energy potentials involved in polyphase systems of more than one media are known only qualitatively, and therefore it is not possible at present to predict quantitatively the characteristic thresholds for vapor condensation on impurities. In any case, the saturation vapor pressure determines the lowest limit of threshold conditions and, accordingly, the Mach number at which vapor saturation is reached will be designated as the minimum threshold Mach number. This limit may easily be found graphically from a pressure-temperature diagram, as it is the Mach number at which the wind-tunnel expansion isentrope crosses the saturation-vapor pressure curve for air.

Theoretically, then, the gain in Mach number of flow without condensation that can be realized by achieving stable supersaturation is limited, at best, to the difference between the maximum and minimum threshold Mach numbers. For example, 4.5 is the minimum threshold Mach number for a reservoir pressure $H_0 = 6$ atmospheres and a reservoir temperature $T_0 = 300^\circ$ Kelvin. Referring to figure 1, the corresponding maximum threshold Mach number is 5.6. Thus, at this reservoir pressure and temperature, the possible gain in Mach number is limited to 1.1. If still higher Mach number flow without condensation is to be produced, increased reservoir temperatures will be necessary. Since it is not always practical to increase the reservoir temperature, it appears desirable to determine whether some condensation in the flow may be tolerated.

Determination of the Properties of a Supersonic Air Stream with Condensed Phase

Ordinarily, supersonic stream properties are uniquely determined by any one stream property and the reservoir conditions. However, where condensation has occurred, it cannot be expected that the usual flow relations are valid. Accordingly, theoretical relationships between possible measurable quantities and the properties of a supersonic air

stream with condensed phase are required. It will be assumed that the vapor phase in such a stream behaves as an ideal gas.² This assumption is consistent with an analysis of the condensation shock process in one-dimensional supersonic flow made by Heybey (reference 14). The analysis rests on the additional assumption that the amount of condensed phase is small enough so that changes in the gas constants and loss of mass from the vapor phase may be neglected compared to the effects of the heat of vaporization which is added to the stream. (This does not seriously restrict the application of the analysis since, as will be seen later, the fraction of condensed phase is, indeed, limited to small values.) With this latter assumption, the effects of condensation are determined using only the equation of state of a perfect gas and the equations representing the conservation of energy, momentum, and mass flow across a shock. These conservation equations must be satisfied by any flow process isolated from external systems; thus the analysis applies to a gradual heat addition process, such as the condensation of air, as well as to a discontinuous process, such as a condensation shock. In addition, the analysis is valid for heat subtraction as well as for heat addition, and may, in fact, be applied to the subsonic case. Therefore, the effects of evaporation of condensed phase in subsonic flow behind a normal shock may be evaluated as well as the effects of condensation or evaporation in supersonic flow.³

Applying Heybey's analysis to the determination of the properties of a partially condensed wind-tunnel air stream, the notation illustrated in figure 2 will be followed. It is assumed that the air stream processes follow the sequence: (a) complete (isentropic) expansion without condensation from the reservoir to station 1; (b) partial condensation of the supersaturated stream in the one-dimensional flow between stations 1 and 2; (c) a compression shock between stations 2 and 3 which

²It is not immediately obvious that this assumption is valid, since the air vapor is in the critical region of liquefaction and condensed phase is present. However, it appears to represent a reasonable approximation because the rate of change of the condensed fraction is limited by the growth rate of small droplets (see, for instance, reference 12) and thus instantaneous changes in the vapor properties will obey an equation of state for a gas. Available equations of state do not deviate seriously from the perfect gas law at the stream conditions considered in the present paper, and using Berthelot's equation of state after the method of Eggers (reference 13) it can be shown that these deviations do not greatly affect the flow.

³More recently Wegener, Stollenwerk, Reed, and Lundquist (reference 4) and Buhler, Jackson, and Nagamatsu (reference 15) have also presented methods by which certain properties of a stream with condensed phase may be calculated. However, Heybey's analysis has the advantage of relative simplicity and completeness.

may be either normal or oblique; and (d) evaporation of condensed phase downstream of the shock⁴ between stations 3 and 4 if the compression caused by the shock results in subsaturated conditions of pressure and temperature. In the case of normal shocks, isentropic deceleration of the subsonic flow at station 4 to zero velocity flow at station 5 is assumed.

Initial stream properties just before condensation occurs (station 1) may be determined with the isentropic expansion equations, provided any one of these properties and the reservoir conditions are known. Between stations 1 and 2, the equations of reference 14 (see equations (C1) through (C6) of appendix C) define the increase in temperature and static pressure and the decrease in Mach number and total pressure of the stream as a function of the initial stream properties and the amount of heat added to the flow. Accordingly, knowing the properties before condensation and any one of the properties of the stream with condensed phase, the amount of heat added to the flow Q and the remaining properties of the stream with condensation may be calculated.

The above discussion outlines the manner in which properties of a supersonic air stream with condensed phase may be deduced from experimental measurements. It is shown in appendix C that the Mach number M_H calculated from the ratio of measured local pitot pressure to reservoir pressure (hereafter designated the pitot Mach number) may be identified as the initial Mach number M_1 of the fully expanded condensation-free flow. Also, the local static pressure p_2 is a property of flow with condensation that can be measured directly. Thus measurements of static pressure, pitot pressure, and reservoir conditions provide sufficient information to determine the properties of a partially condensed air stream.

A graphical determination of certain of the stream properties is more convenient than an analytic solution in view of the form of the relations which are involved. The pressure-temperature diagram (fig. 3) illustrates how such a graphical solution may proceed. The expansion isentrope for the supersonic wind-tunnel flow is followed on this diagram until the measured pitot Mach number is reached. This point represents the flow at station 1. As condensation proceeds, the static pressures and temperatures follow a path, defined by equations (C2) and (C3) of appendix C, which is designated as a line of compression due to heat addition in figure 3. This path is followed until the measured static pressure p_2 is reached and this point represents the flow at station 2.

⁴The assumption that evaporation takes place downstream of the shock is for the purpose of convenience only. It is noted that the change in heat content may be accounted for by adding an equivalent term to the equation of energy continuity in the usual analysis of the shock process, and the point at which the energy change occurs makes no difference to the final result.

The heat added to the flow Q and the Mach number M_2 can be evaluated from the grid of constant Mach number and constant heat addition lines, and the static temperature T_2 is, of course, the abscissa of this point on the temperature scale. Remaining stream properties at station 2 can be calculated from their values at station 1 and the value of Q .

The errors introduced by neglecting the loss of mass from vapor phase are considered in appendix C and are found to be the same order of magnitude as the fraction of condensed phase. For the case considered in figure 3, the amount of heat added to the stream, up to initial Mach numbers of 6, is limited to about 3 calories per gram of air or less. This corresponds to fractions of condensed air of 6 percent or less.

It may be noted that as a consequence of the decrease in total pressure as condensation proceeds in a supersonic stream (given by equation (C4) of appendix C), the Mach number M_p determined from the ratio of static to reservoir pressure is not the stream Mach number (hereafter M_p is designated the static Mach number). However, the ratio of static pressure to pitot pressure at the same point in the air stream determines a Mach number M_{pH} (designated the pitot-static Mach number) which, to an accuracy consistent with the assumptions of this analysis, is the stream Mach number M_2 at that point. This results because subtraction of heat, due to evaporation of condensed phase, has a negligible effect on the total pressure in the flow downstream of the normal shock. (See appendix C.) Consequently, the pitot pressure H_5 is essentially the same as the total pressure behind the normal shock H_3 and may be substituted for this quantity in the Rayleigh formula determining M_2 .

It will be recalled it was assumed that condensation occurs in the wind-tunnel flow at Mach number M_1 after expansion is complete. Since condensation may begin during the expansion process at some Mach number between the minimum threshold Mach number and M_1 , some justification for this assumption is appropriate. The assumption that condensation occurs at M_1 actually corresponds to one limiting case, while the other limit would be represented by condensation just sufficient to maintain saturation conditions of air as the stream is expanded beyond the minimum threshold Mach number. Calculations (based on equations (C1) through (C6) of appendix C) show that the latter limiting process requires a greater increase in enthalpy to achieve the same measured stream static pressure and pitot pressure, but that the other stream properties derived are essentially the same in either case. Consequently, the method of analysis which assumes condensation at M_1 may be expected to yield reasonably accurate values of all pertinent stream properties with the possible exception of Q and enthalpy, which may be underestimated.

Determination of Some Effects of Local Regions
of Evaporation and Condensation in
Flow About Models

It will be assumed that the properties of a partially condensed supersonic air stream may be determined with adequate accuracy by the methods discussed previously; then the behavior of flow about models immersed in such a stream can be investigated.

Evaporation of condensed phase in local compression regions and increased condensation in local expansion regions are expected to affect the flow properties in these regions. Consider the compression over a flat surface at positive angles of attack. The flow downstream of the bow shock is essentially one-dimensional and, if it is assumed that no interaction between evaporation of condensed phase and the shock process occurs, the changes in properties of the flow downstream of the shock may be calculated using an analysis similar to that described in the preceding section. A graphical solution of the pressures and temperatures in this region may be found on a diagram similar to figure 3. A point representing the flow immediately downstream of the compression shock process (station 3, fig. 2) is first located. If this point is in the subsaturated domain of pressure and temperature, a path of heat subtraction is then followed until the saturation line of air is reached or until an amount of heat has been subtracted from the stream corresponding to evaporation of all the condensed phase initially present in the air stream. The path of heat subtraction is similar to a line of compression due to heat addition, being defined by the same equations but using negative values for the heat added Q and conditions at station 3 for the initial stream properties.

In the case of expansion regions over a flat surface at negative angles of attack, the processes that may ensue subsequent to or during the expansion are not as clearly evident, as in the case of compression, for the same reasons that the mechanism of condensation is in doubt. For example, if the point on the pressure-temperature diagram representing flow immediately after the expansion is in the supersaturated domain, and if condensation has not been initiated in the stream ahead of the expansion, the additional supersaturation introduced may still be stable. However, if condensation has been initiated in the free stream, the amount of condensed phase will increase until the saturation line of air is reached along a heat-addition path.

It should be noted that evaporation and/or condensation processes may exhibit some time lag. Thus the changes in flow properties just discussed are more properly limiting changes that are approached as the flow proceeds along the surface.

EXPERIMENTS ON CONDENSATION PHENOMENA AND DISCUSSION OF RESULTS

The experiments on condensation phenomena were divided into tests concerning (a) condensation in supersonic wind tunnels and (b) flow about models in a supersonic air stream containing some condensed air. The early tests were conducted in the Ames 10- by 14-inch supersonic wind tunnel. Further investigations of the condensation phenomena using various supply media were conducted in a 1- by 1.4-inch supersonic nozzle.

Wind Tunnels

A detailed description of the Ames 10- by 14-inch supersonic wind tunnel is reported in reference 16. All the tests in this tunnel were made with a reservoir pressure of approximately 6 atmospheres and a reservoir temperature of approximately 288° K. The static and pitot pressure probes and test models were located 48 inches downstream of the sonic throat.

The 1- by 1.4-inch supersonic nozzle is essentially a 1/10-scale model of the 10- by 14-inch supersonic wind tunnel (see fig. 4(a)). All tests in this nozzle were conducted with a reservoir pressure of approximately 6 atmospheres. The pressure probes were located 5-1/2 inches downstream of the sonic throat. Figure 4(b) shows the arrangement of equipment with a heater and a cold trap in the normal supply air line to the nozzle. The 2-kilowatt Cal-Rod heater was used to vary the reservoir temperature between 300° K and 450° K. The cold trap was surrounded by a dry ice and acetone bath and primarily served to reduce the water-vapor content of the supply air.⁵ To facilitate the investigation of various supply gases, a high pressure manifold connected ten compressed gas cylinders to the nozzle supply line (see fig. 4(c)). The reservoir pressure was again maintained at approximately 6 atmospheres by throttling through a needle valve; this throttling reduced the reservoir temperature to about 278° K.

⁵In addition, an electrostatic precipitator was used in a few tests to reduce the concentration of silica gel and dust in the supply air. An appreciable fraction of these particles passed through the precipitator, however, so the tests were inconclusive with respect to the consequences of such purification. The precipitator design used gave a corona charging current density of 0.06 milliamperes per square inch normal to the flow, which had a velocity less than 0.6 feet per second; 20 kilovolts were applied to a 10 inch long aluminum plate collector unit.

Instrumentation and Models

The theoretical considerations of condensation phenomena indicated that the properties of a stream containing small amounts of condensed phase can be determined if reservoir conditions and both local static and pitot pressures are known. Therefore, these properties were measured in the 10- by 14-inch supersonic wind tunnel and the 1- by 1.4-inch supersonic nozzle air streams. In the tests conducted in the 10- by 14-inch supersonic wind tunnel the reservoir pressures were measured with a Bourdon type gage and the reservoir temperatures were measured with an iron-constantan thermocouple and an automatic temperature recorder. The static pressures were measured with a static pressure probe and McLeod type gage. The static pressure probe was a 10° apex angle, cone-cylinder combination having a 1/8-inch outside diameter and four equally spaced orifices located 16 diameters from the apex of the cone. This probe geometry gave the most accurate results according to reference 17. Tests using probes of the same geometric shape with orifices located 16, 20, and 24 diameters from the apex of the cone yielded a negligible variation in static pressure. The pitot pressures were measured on a U-tube-type manometer which was connected to a flat-faced, 1/4-inch outside-diameter pitot pressure tube with an outside-to-inside diameter ratio of 1.5. Tests using several pitot probes having diameter ratios from 1.5 to 10 revealed no measurable changes in pitot pressure.

Two sting-supported pressure-distribution models were constructed to test the effects of local regions of evaporation and/or condensation about bodies: a 10° wedge of 4-inch span with pressure orifices 2 inches from the leading edge; and a 10-caliber ogive-cylinder combination, 1 inch in diameter and 10 inches long, with pressure orifices distributed along its length.

The static and pitot pressure probes that were used in the 1- by 1.4-inch supersonic nozzle were geometrically similar to those used in the 10- by 14-inch supersonic wind tunnel; the outside diameters were 0.050 inch. The reservoir pressures and temperatures were measured in the same manner as in the larger tunnel.

Water content of the compressed gases used to operate the 1- by 1.4-inch nozzle was determined with a cooled-mirror-type dew-point indicator.

Results and Discussion

Flow in supersonic wind tunnels. - Tests in the Ames 10- by 14-inch supersonic wind tunnel yielded pitot Mach numbers M_H , static Mach numbers M_p , and pitot-static Mach numbers M_{pH} as shown in figure 5.

The scatter in pitot and static Mach numbers was less than ± 0.02 and the scatter of pitot-static Mach numbers was about ± 0.04 . These three Mach numbers agree at values lower than the threshold Mach number, $M^* = 4.4$, but deviate from each other at values greater than M^* due to condensation of air. The pitot-static Mach number, which was shown theoretically to be approximately the Mach number of the stream, increases very slowly beyond the threshold Mach number as the wind-tunnel expansion is increased.

Further evidence that condensation occurs at Mach numbers greater than M^* was obtained by observation of light scattering in the wind-tunnel test section similar to that reported in reference 3. The arrangement used to obtain photographs of the light scattering is illustrated in figure 6. Photographs showing the presence of light scattering at a Mach number above threshold and the absence of light scattering at a Mach number below threshold are presented in figures 7(a) and 7(b). The light scattering is just visible at the threshold Mach number as determined by pressure measurements; thus it serves as a fairly sensitive indicator of the presence of condensed phase.

At the threshold Mach number, the values of stream static pressure and temperature in the 10- by 14-inch supersonic wind tunnel correspond very closely to those of saturated air (i.e., no appreciable supersaturation occurs). This result indicates that large concentrations of effective nuclei are present in the normal supply air. In addition to approximately 0.03 percent by volume of carbon dioxide and about 0.005 percent by volume of residual water vapor, both of which are possible sources of nuclei, this air contains silica gel particles up to 100 microns in diameter. These particles are sufficiently small to pass through filters downstream of the silica gel towers in which the air is dried.

In order to investigate whether carbon dioxide, water vapor, or silica gel particles may form the effective nuclei, further tests were made using some purified gases. It was not practical to perform these experiments in the large-scale wind tunnel; hence they were conducted in the 1- by 1.4-inch supersonic nozzle. In addition to the normal supply air, which was heated to various temperatures, the following three gases were used as supplies for the nozzle:

1. Compressed nitrogen, which was relatively free of possible sources of foreign nuclei.
2. Dry compressed air, which contained the usual amount of carbon dioxide, but which was relatively free of silica gel particles and contained only about 0.0003 percent by volume of water vapor.
3. Normal supply air passed through a cold trap. This air contained the usual concentrations of carbon dioxide and silica gel particles but the water content was reduced from about 0.005 to 0.0003 percent by volume.

Representative static and pitot Mach numbers obtained from the tests in the 1- by 1.4-inch nozzle are presented in figures 8(a) and 8(b) as a function of Mach number from nozzle area ratio. These Mach numbers are shown for the different gas supplies at various reservoir temperatures and, though the scatter in these data is as much as ± 0.08 in Mach number, they exhibit the same characteristics as those obtained from the 10- by 14-inch supersonic wind tunnel. The pitot-static Mach numbers are not shown; however, in each case, this Mach number increases very slowly with increasing nozzle-area ratio after the threshold Mach number is exceeded.

The threshold Mach numbers are of primary concern here, and these are presented in figure 9 as a function of reservoir temperature. It is seen that at normal reservoir temperatures the normal supply air in the 1- by 1.4-inch nozzle gives an M^* agreeing with that found in the 10- by 14-inch supersonic wind tunnel (i.e., very close to the theoretical minimum). At high reservoir temperatures an M^* somewhat less than the theoretical minimum is indicated for this air. This discrepancy is believed due to the heat transfer from the hot air to the relatively cool walls of the nozzle in the region of the sonic throat, thus yielding a stream stagnation temperature less than that measured in the reservoir. The nitrogen and the dry compressed air give threshold Mach numbers higher than the theoretical minimum threshold for air by about 70 percent of the possible increase in threshold Mach number predicted by the Becker-Döring theory. At both low and high reservoir temperatures, the normal supply air which was dried with the cold trap gives threshold Mach numbers higher than those obtained using undried air by about 20 percent of the theoretically attainable increase. These results suggest that water vapor may form embryos that are effective condensation nuclei in air which is saturated, that silica gel particles may serve as condensation nuclei in air which is slightly supersaturated, and that small amounts of carbon dioxide do not form effective nuclei for air, at least until rather high degrees of supersaturation are reached.⁶ This result could be due to the time lag of formation of carbon dioxide nuclei (appendix B).

Results of experiments reported in reference 4 are also shown in figure 9. The reservoir pressures are not identically 6 atmospheres for

⁶In this connection, carbon dioxide was added to the normal supply air in the reservoir of the 10- by 14-inch supersonic wind tunnel. At Mach numbers just above threshold the amount of light scattering in the test section was markedly reduced. A few observations were made at higher Mach numbers and no change in the apparent amount of condensation was detected by either light scattering or pressure measurements. These results appear to be inconsistent with the hypothesis that carbon dioxide does form effective nuclei. However, in view of some experiments reported by Nagamatsu (reference 18) which appear to support this hypothesis, the subject evidently needs further investigation.

these tests but, since M^* is relatively insensitive to reservoir pressures, the value of the comparison is not seriously affected. The degree of supersaturation indicated by the data of reference 4 is observed to be in agreement with that obtained in the 1- by 1.4-inch supersonic nozzle with the dry compressed air.

The variations of static pressure with static temperature in the 10- by 14-inch supersonic wind tunnel and in the 1- by 1.4-inch supersonic nozzle are shown in figures 10(a) and 10(b). The threshold Mach numbers are indicated by the slope discontinuities caused by the onset of condensation. At Mach numbers less than M^* the pressure-temperature relation is the usual expansion isentrope. For Mach numbers greater than M^* the air-stream static temperatures were determined graphically using pressure-temperature diagrams similar to figure 3. With the normal supply air the stream properties follow the saturation conditions for air⁷ when threshold conditions are exceeded, while the purified gases yield static conditions well into the supersaturated domain of pressure and temperature. The nitrogen and dry compressed air achieve considerable supersaturation before condensation begins, but once initiated, condensation proceeds to bring stream conditions closer to saturation.

Flow about models.— In the section Theoretical Considerations a method was outlined for estimating the properties of flow about plane, two-dimensional models in a supersonic stream with condensed phase. This method has been used to calculate the pressures on an inclined flat surface in the 10- by 14-inch supersonic wind-tunnel air stream. For comparison, pressures were measured on the surfaces of the wedge model with the surface planes at angles of attack from 0° to 10° . At the Mach numbers where condensation is encountered in this stream, the pressures on surfaces at negative angles of attack are low and contribute little to the total forces exerted on the model, therefore no tests were conducted with a model surface in this attitude.

Figure 11 shows the ratio of surface pressure to free-stream static pressure as a function of angle of attack of the surface for several free-stream Mach numbers. Two theoretical curves are presented: the solid curve is for oblique shock theory with a correction for a laminar boundary

⁷ Static temperatures calculated from the data for the high reservoir temperature tests are apparently in error by about 5 percent. Again, this error may be due to the heat transfer from the air to the nozzle walls in the region of the sonic throat. Being consistent, the error does not affect the comparison between the air with and without extra drying by cold trap.

layer,⁸ and the dashed curve incorporates the additional correction for evaporation of condensed phase in air passing through the oblique shock. The experimental data clearly fall below the theory without correction for evaporation and approach agreement with the corrected theory at the higher Mach numbers. At a Mach number of 4.48, just above threshold, the fraction of condensed phase is extremely small and hence the reduction in pressure due to evaporation is small (see fig. 11(a)). At higher Mach numbers, however, the extent of condensation increases and the reduction in pressures becomes rather large. To show this Mach number effect more clearly, the pressure ratios for the surface at 5° angle of attack are presented in figure 12 as a function of free-stream Mach number. A curve of the pressure ratios calculated from oblique shock theory, without further corrections, is also included in figure 12. It is of interest to note that the pressure changes due to evaporation of condensed phase may be the same order of magnitude as the pressure correction for the compressible, laminar boundary layer. The pressures measured at Mach numbers less than threshold and at zero angle of attack at all Mach numbers are evidence justifying the laminar-boundary-layer correction.

Figure 13 presents further evidence that the condensed phase evaporates behind the compression shock produced by the surface at 5° angle of attack. This figure is a photograph of the light scattering from a beam of slit aperture which intersects the flow about the 4-inch-span wedge model. (The light beam traverses the stream perpendicular to the flow as shown in figure 6. A shield was used to eliminate the reflection from the near window.) Light scattering disappears almost immediately behind the shock wave, which implies not only that evaporation occurs but that the time lag is negligible.

In order to investigate the effects of both evaporation and condensation in the local flow field about a model of more arbitrary shape, pressures were measured along the surface of a 10-caliber ogive cylinder ($\alpha = 0^\circ$, $M_{\infty} = 4.67$). Figure 14 presents the experimental data and a theoretical pressure distribution, uncorrected for the boundary-layer displacement thickness, taken from reference 20. The agreement between the theory and the experimental data along the ogive portion of the body is believed due to the compensating effects of the decrease in pressure caused by evaporation and the increase in pressure associated with the boundary layer. This compensation is not surprising in view of the

⁸The pressures were calculated for flow deflections equal to the sum of the angle of attack of the model surface and the angular slope of the boundary-layer displacement thickness relative to this surface. The slope of the boundary-layer displacement thickness was found using the results of Monaghan (reference 19).

results found in the case of the flat surface (see fig. 12). Along the cylindrical portion of the body there seems to be no detectable effect of recondensation.

These observations are supplemented by photographs of light scattering at several stations along the model shown in figure 15. In figure 15(a) the light beam intersects the model near the junction of the ogive and cylinder, 2.5 body diameters from the nose, but no light scattering is visible inside the shock even though the stream near the body is theoretically supersaturated. This implies not only that evaporation has occurred downstream of the nose shock, but also that there is some time lag in the development of condensed phase. At a distance of 5 body diameters from the nose (fig. 15(b)) some light scattering inside the shock is noticeable and this feature becomes more pronounced with increasing distance downstream, indicating that the amount of condensed phase increases with time and that the time lag mentioned above is of the order of 40 microseconds (figs. 15(c), (d), and (e)). As expected, the high temperature boundary-layer region is characterized by the absence of light scattering and the flow region near the shock contains less condensed phase than the region of more expanded flow nearer the model.

CONCLUSIONS

1. The Mach number of supersonic flow in wind tunnels cannot be increased greatly beyond the threshold Mach number by increasing the nozzle area ratio. The threshold Mach number may be increased by obtaining supersaturated conditions in the stream, but the possible gain in Mach number range is small and relatively elaborate means of air purification are required to achieve this gain. Therefore, elevating the reservoir temperature to maintain subsaturated stream conditions appears the most practical method of increasing the Mach number range of supersonic wind tunnels.

2. By use of the relations originally developed by Heybey for condensation shock processes, the properties of a supersonic air stream with a small fraction of condensed phase may be evaluated from measured reservoir conditions, stream static pressure, and stream pitot pressure. Within the accuracy of this analysis, the stream Mach number is determined by the ratio of static to pitot pressure and the Rayleigh formula.

3. The properties of flow about wedge models in a partially condensed supersonic air stream may be determined approximately. Evaporation of condensed phase can significantly alter the model surface pressures; therefore, the presence of condensed phase in a supersonic air stream used for model tests is undesirable.

4. Scattering of light from droplets of condensate is a sensitive indicator of the presence of enough condensed phase to affect stream

properties. According to light scattering observations, the condensation processes exhibit a time lag in approaching equilibrium after a change in stream conditions, but the time delay is comparatively small in the evaporation caused by compression through a shock wave.

Ames Aeronautical Laboratory
National Advisory Committee for Aeronautics
Moffett Field, Calif., Feb. 13, 1952

APPENDIX A

CALCULATION OF THE THEORETICAL MAXIMUM
AND MINIMUM THRESHOLD MACH NUMBERS

The saturation vapor pressure of air is assumed to be the pressure of a perfect liquid or solid solution of oxygen and nitrogen in equilibrium with a 20-percent-oxygen, 80-percent-nitrogen vapor. Then the volume fraction of liquid-phase oxygen X_{O_2} in this solution is:

$$X_{O_2} = \frac{1}{1+4 \frac{p_{O_2}}{p_{N_2}}} \quad (A1)$$

and the saturation vapor pressure of air p_∞ is:

$$p_\infty = X_{O_2} p_{O_2} + (1-X_{O_2}) p_{N_2} \quad (A2)$$

where p_{O_2} is the vapor pressure of pure oxygen and p_{N_2} the vapor pressure of pure nitrogen, both being functions of temperature given in the NBS-NACA tables (reference 21). Where necessary, these data were extrapolated to temperatures lower than those given in reference 21 with the equations from Henning and Otto (reference 22).

The saturation vapor pressure of air is used to calculate the nucleation rate J from the equation derived by Becker and Döring (reference 6):

$$\log J = A + 2x + 2 \log x - \frac{B}{x^2} \quad (A3)$$

where

$$A = 22 + \log \frac{p_\infty^2 d}{\lambda_s (mS)^{3/2}}$$

$$B = 1.45 \left(\frac{S}{T} \right)^3 \left(\frac{m}{d} \right)^2$$

d = density of condensed phase (gm/cc)

$x = \log p/p_\infty$

λ_s = mean free path in vapor phase at standard pressure and temperature (cm)

m = gram molecular weight of vapor phase

S = surface tension of a condensate droplet of critical radius (dyne/cm)

The value of liquid-air density d and bulk liquid surface tension S_∞ are calculated from the values for oxygen and nitrogen tabulated by Landoldt-Börnstein (reference 23). According to Tolman (reference 7), the surface tension S of a droplet of critical radius r_c is:

$$S = \frac{S_\infty}{1 + \frac{2\delta}{r_c}} \quad (A4)$$

where δ is approximately one-half the radius of a liquid molecule and the critical radius r_c is given by the Thomson formula (see reference 6 or 10):

$$r_c = \frac{0.868 Sm}{RTd \log p/p_\infty} \quad (A5)$$

or, using equation (A4),

$$r_c = \frac{0.868 S_\infty m}{RTd \log p/p_\infty} - 2\delta \quad (A5a)$$

All the variables in equation (A3) can be expressed as a function of static temperature which, in turn, is a function of Mach number. The nucleation frequency $J = 10^{12}$ was chosen as the criterion for the threshold of condensation and, accordingly, determines a maximum threshold Mach number.

The Mach number at which the pressure and temperature of the wind-tunnel expansion isentrope satisfies the saturation vapor pressure function p_∞ is, of course, the minimum threshold Mach number.

APPENDIX B

EMBRYO GROWTH RATES OF CARBON DIOXIDE
AND WATER VAPOR IN AIR

The mean time t between collisions of two vapor particles is the ratio of the mean free path to the mean velocity of the particles $t = \lambda/\bar{v}$. From kinetic theory, the mean free path λ is:

$$\lambda = \frac{1}{\sqrt{2 \pi L \sigma^2}}$$

and the mean velocity \bar{v} is:

$$\bar{v} = \sqrt{\frac{8kT}{w\pi}}$$

where

L number of particles per unit volume (cc^{-1})

σ diameter of a particle (cm)

w mass of particle (gm)

For a vapor impurity that is highly supersaturated the accommodation coefficient of the collisions is assumed to be unity (i.e., particles are always united by each collision). It is also assumed that the impurity remains homogeneous in particle size. Then after a time t the vapor particles have a density L' , diameter σ' , and mass w' given by:

$$L' = L/2$$

$$w' = 2w$$

$$\sigma' = 2^{1/3}\sigma$$

Then the mean time t' to the succeeding collision will be $t' = 2^{5/6}t$ and after $(n-1)$ collisions, the mean time t_n to the nth collision will be:

$$t_n = (2^{5/6})^{n-1} t_1$$

where t_1 is the mean time of the first collision of single vapor molecules.

The total time T_n of n collisions is:

$$T_n = t_1 \sum_{i=0}^n (2^{5/6})^i = t_1 \left(\frac{1-2^{5n/6}}{1-2^{5/6}} \right)$$

The number of molecules g in the aggregate after time T_n is $g = 2^n$ and the diameter of the aggregate is $\sigma = g^{1/3} \sigma_1$ where σ_1 is the molecular diameter.

These results are now applied to the case of air expanded to a Mach number of 5 from a reservoir pressure of 6 atmospheres and a reservoir temperature of 300° K. Let $T_n = 6 \times 10^{-3}$ seconds (approximately the time of flow from sonic throat to test section of the 10- by 14-inch super-sonic wind tunnel). Then for air that contains 0.0003 volume fraction of carbon dioxide the diameter of the resulting embryos of carbon dioxide is:

$$\sigma_{CO_2} = 48 \times 10^{-8} \text{ cm}$$

and for air that contains 0.00005 volume fraction of water vapor the diameter of the resulting embryos of water is:

$$\sigma_{H_2O} = 28 \times 10^{-8} \text{ cm}$$

For comparison, the critical diameter $2r_c$ of condensate required for self-nucleation may be calculated from Thomson's formula (equation (A5)):

$$2r_c = 22 \times 10^{-8} \text{ cm}$$

The size of the carbon dioxide and water embryos is the same order of magnitude as the critical nuclei size. Thus it appears that time intervals of the magnitude of those available in wind-tunnel flow may be required before these concentrations of carbon dioxide and water vapor can grow embryos of sufficient size to serve as condensation nuclei.

APPENDIX C

EFFECTS OF CONDENSATION AND EVAPORATION

ON THE PROPERTIES OF AN AIR STREAM

The effect of adding heat to supersonic flow may be calculated from the equations given in reference 14. Using the notation of this paper,

$$\frac{M_2}{M_1} = \frac{u_2}{u_1} \left(\frac{1 - \frac{\gamma-1}{\gamma+1} u_1^2}{1 - \frac{\gamma-1}{\gamma+1} u_2^2} \right)^{\frac{1}{2}} \quad (C1)$$

$$\frac{p_2}{p_1} = \xi \frac{u_2}{u_1} \left(\frac{M_1}{M_2} \right)^2 \quad (C2)$$

$$\frac{T_2}{T_1} = \left(\xi \frac{u_2}{u_1} \frac{M_1}{M_2} \right)^2 \quad (C3)$$

$$\frac{H_2}{H_1} = \xi \frac{u_1}{u_2} \left(\frac{M_2}{M_1} \frac{u_1}{u_2} \right)^{\frac{2}{\gamma-1}} \quad (C4)$$

where

$$u_2 = \frac{1 + u_1^2 + \sqrt{(1+u_1^2)^2 - 4\xi^2 u_1^2}}{2\xi u_1} \quad (C5)$$

$$\xi^2 = 1 + \frac{Q}{i_0} \quad (C6)$$

and from the supersonic flow relations

$$u_1 = \frac{(\gamma+1) M_1^2}{2 + (\gamma-1) M_1^2}$$

Now across a normal shock:

$$u_2 u_3 = 1 \quad (C7)$$

and if the enthalpy decrease due to evaporation in flow through the shock equals the enthalpy increase in the supersonic flow due to condensation:

$$u_4 = \frac{1 + u_3^2 - \sqrt{(1+u_3^2)^2 - 4\xi^2 u_3^2}}{2\xi^2 u_3} \quad (C8)$$

and

$$\xi^2 = 1 - \frac{Q}{i_0 + Q} = \frac{1}{\xi^2} \quad (C9)$$

The remaining subsonic flow relations are the same as in supersonic flow with a change in subscripts; subscript 1 becomes 3 and subscript 2 becomes 4. Substituting equation (C7) into (C8) and combining with equation (C5) there results:

$$u_1 u_4 = 1 \quad (C10)$$

Equation (C10) expresses the same relation between supersonic and subsonic flow which a normal shock at Mach number M_1 would give. This result could have been foreseen since an entropy jump is uniquely determined by initial supersonic stream conditions if energy, mass, and momentum are conserved. Thus there is no distinction between a single discontinuity and a sequence of nonisentropic processes which satisfies these same conservation requirements.

To the accuracy of the foregoing analysis, then, the total pressure measured by a pitot tube is independent of the amount of condensation, and the ratio of pitot to reservoir pressure (H_5/H_0) determines an initial stream Mach number M_1 that would exist if no condensation occurred.

Where the fraction of condensed phase is small, the measured pitot pressure H_5 may also be used with the measured static pressure p_2 to determine the free-stream Mach number M_2 . This occurs because the heat subtracted from the stream Q is a small fraction of the specific enthalpy in the subsonic flow and the total pressure is not appreciably changed by this decrease in heat content. Thus H_5/H_3 is essentially unity (theoretically H_5/H_3 differs from unity by 0.5 percent in the most extreme case encountered in this investigation) and the measured pitot pressure may be substituted for H_3 in the Rayleigh formula:

$$\frac{p_2}{H_3} = \left[\frac{(\gamma+1) M_2^2}{2} \right]^{\frac{-\gamma}{\gamma-1}} \left[\frac{2\gamma M_2^2 - (\gamma-1)}{\gamma + 1} \right]^{\frac{1}{\gamma-1}} \quad (C11)$$

The order of magnitude of the error involved in the analysis due to the neglect of the momentum and mass removed from the vapor-phase stream was investigated by modifying the mass-flow and momentum equations to represent continuity of the fraction of air which does not condense:

$$\rho_1 (1-\epsilon) V_1 = \rho_2 V_2 \quad (C12)$$

$$(1-\epsilon) p_1 + \rho_1 (1-\epsilon) V_1^2 = p_2 + \rho_2 V_2^2 \quad (C13)$$

where ϵ is the fraction of air condensed. The Mach number and temperature ratios which result from an analysis using equations (C12) and (C13) rather than those for $\epsilon = 0$ have the same formal relation given by equations (C1) and (C3). The static pressure and total pressure ratios are modified, however, by a factor $(1-\epsilon)$:

$$\frac{p_2}{p_1} = (1-\epsilon) \xi \frac{u_2}{u_1} \left(\frac{M_1}{M_2} \right)^2 \quad (C2a)$$

$$\frac{H_2}{H_1} = (1-\epsilon) \xi \frac{u_1}{u_2} \left(\frac{M_2 u_1}{M_1 u_2} \right)^{\frac{1}{\gamma-1}} \quad (C4a)$$

The ratio u_2 is the same function of u_1 as given in equation (C5), hence the Mach number and static temperature are not affected by this correction, but the static pressure and total pressure are in error by ϵ .

REFERENCES

1. Hermann, R.: Condensation Shock Waves in Supersonic Wind Tunnel Nozzles. British M.A.P., R.T.P. Trans. No. 1581.
2. Bogdonoff, S. M., and Lees, L.: Study of the Condensation of the Components of Air in Supersonic Wind Tunnels. Pt. I. Absence of Condensation and Tentative Explanation. Princeton University, Aero. Engineering Lab. Rept. 146, May 1949.
3. Becker, J. V.: Results of Recent Hypersonic and Unsteady Flow Research at the Langley Aeronautical Laboratory. Jour. of Appl. Phys., vol. 21, 1950, p. 619.
4. Wegener P., Stollenwerk, E., Reed, S., and Lundquist, G.: NOL Hyperballistics Tunnel No. 4 Results I: Air Liquefaction. NAVORD Rept. 1742, Jan. 1951.
5. Buhler, Rolf D.: Recent Results on the Condensation Investigation. Guggenheim Aero. Lab., Calif. Inst. Tech., July 1950.
6. Becker, R., and Döring, W.: Kinetische Behandlung der Keimbildung in Übersättigten Dämpfen. Ann. der Physik, vol. 24, 1935, p. 719.
7. Tolman, R. C.: Effect of Droplet Size on Surface Tension. Jour. Chem. Phys., vol 17, 1949, p. 333.
8. Stever, H. Guyford, and Rathbun, Kenneth C.: Theoretical and Experimental Investigation of Condensation of Air in Hypersonic Wind Tunnels. NACA TN 2559, 1951.
9. Durbin, Enoch J.: Optical Methods Involving Light Scattering for Measuring Size and Concentration of Condensation Particles in Supercooled Hypersonic Flow. NACA TN 2441, 1951.
10. Frenkel, J.: Kinetic Theory of Liquids. Oxford Press, ch. VII, 1946.
11. Schaefer, Vincent J.: The Formation of Ice Crystals in the Laboratory and the Atmosphere. Chem. Rev., vol. 44, no. 2, April 1949, pp. 291-320.
12. Hazen, Wayne E.: Some Operating Characteristics of the Wilson Cloud Chamber. Review of Scientific Instruments, vol 13, June 1942, pp. 247-252.
13. Eggers, A. J., Jr.: One-Dimensional Flows of an Imperfect Diatomic Gas. NACA Rep. 959, 1950. (Formerly NACA TN 1861)

14. Heybey: Analytical Treatment of Normal Condensation Shock.
NACA TM 1174, July 1947.
15. Buhler, Rolf, Jackson, Paul, and Nagamatsu, H. T.: Oblique Shock Waves with Evaporation; Method of Calculating Free Stream Temperature and Amount of Condensation from Wedge Tests; Remarks on the Pressure Coefficient in Hypersonic Tunnels. Guggenheim Aero. Lab., Calif. Inst. Tech., Memorandum No. 3, April 1951.
16. Stevens, Victor I.: Hypersonic Research Facilities at the Ames Aeronautical Laboratory. Jour. of Appl. Phys., vol. 21, 1950, p. 1150.
17. McLellan, C. H., Williams, T. W., and Beckwith, I. E.: Investigation of the Flow Through a Single-Stage Two-Dimensional Nozzle in the Langley 11-Inch Hypersonic Tunnel. NACA TN 2223, 1950.
18. Nagamatsu, Henry T.: Hypersonic Wind Tunnel Bimonthly Progress Summary, Feb. 1, 1951 to April 1, 1951. Guggenheim Aero. Lab., Calif. Inst. Tech.
19. Monaghan, R. J.: An Approximate Solution of the Compressible Laminar Boundary Layer on a Flat Plate. TN No. Aero. 2025, Sup. 96, R.A.E., Nov. 1949.
20. Rossow, Vernon, J.: Applicability of the Hypersonic Similarity Rule to Pressure Distributions Which Include the Effects of Rotation for Bodies of Revolution at Zero Angle of Attack.
NACA TN 2399, 1951.
21. NBS-NACA Tables of Thermal Properties of Gases. Tables 9.50 and 11.50. U. S. Dept. of Commerce, National Bureau of Standards.
22. Henning, F., and Otto, J.: Damfdrückkurven und Tripelpunkte in Temperaturgebiet von 14° K - 90° K. Phys. Zeits., vol. 37, 1936, p. 633.
23. Landolt-Börnstein: Physikalische-Chemische Tabellen, vol. 1, 1923.

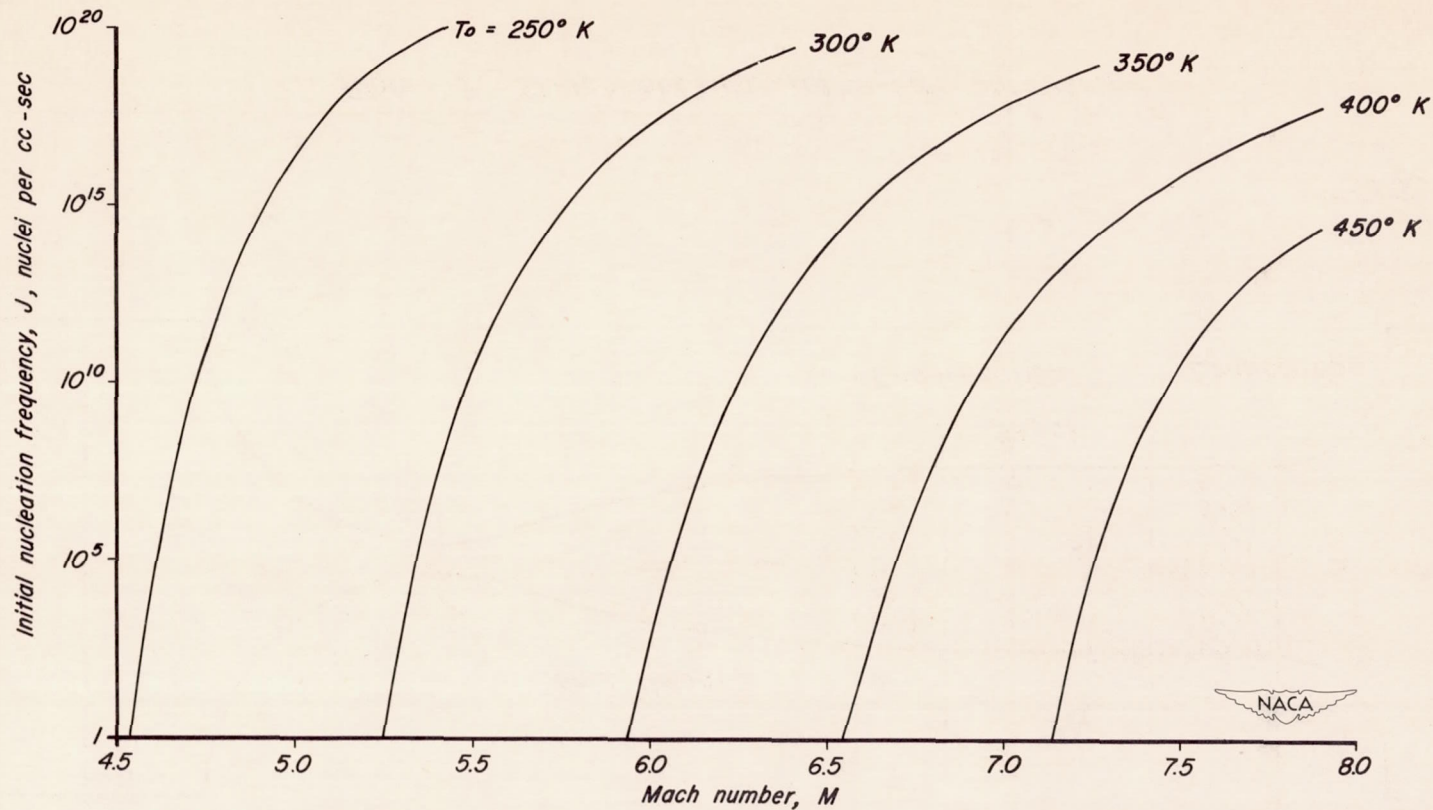


Figure 1.—Initial nucleation frequency as a function of free-stream Mach number with reservoir temperature as parameter.
 $H_0 = 6$ atmospheres.

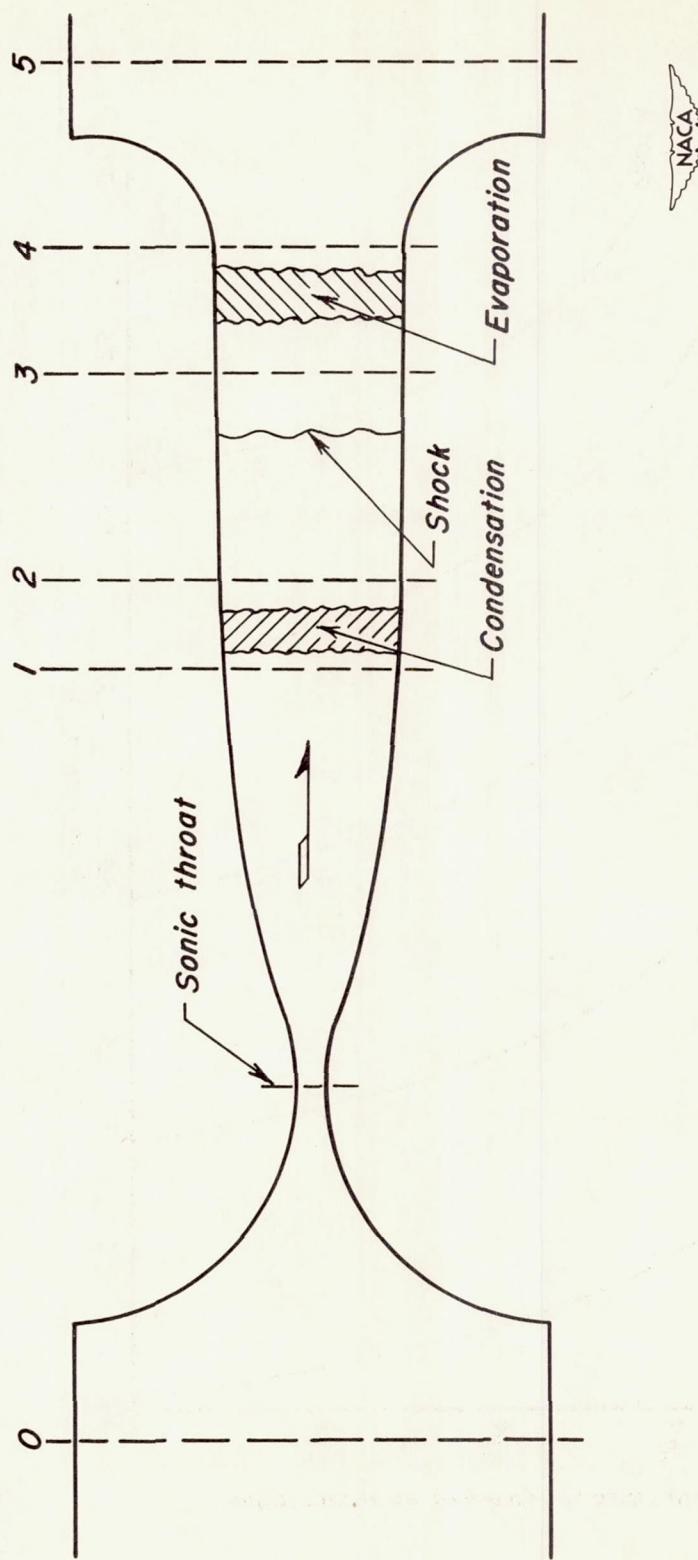


Figure 2.—Sketch showing stream-tube notation.

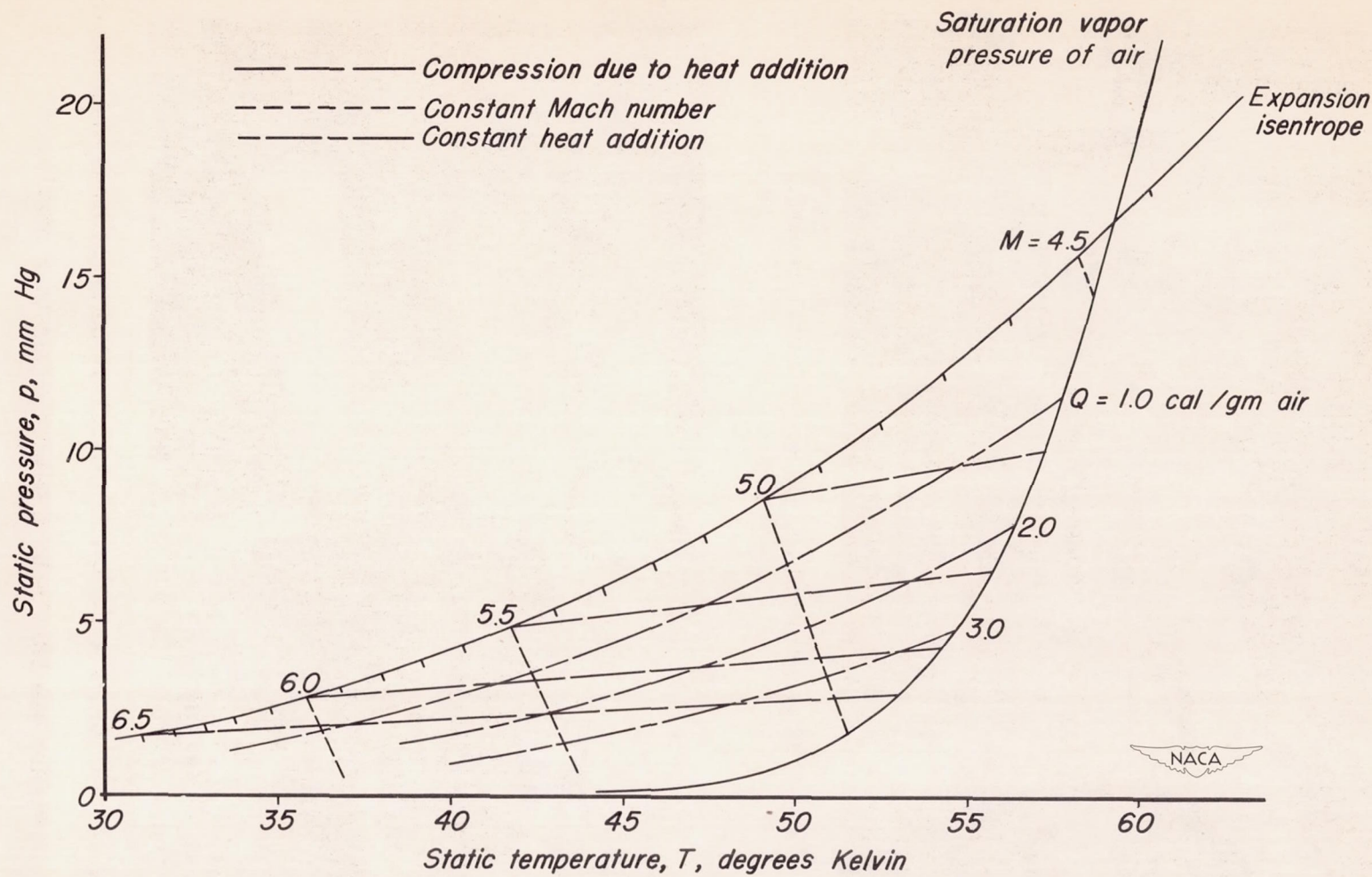
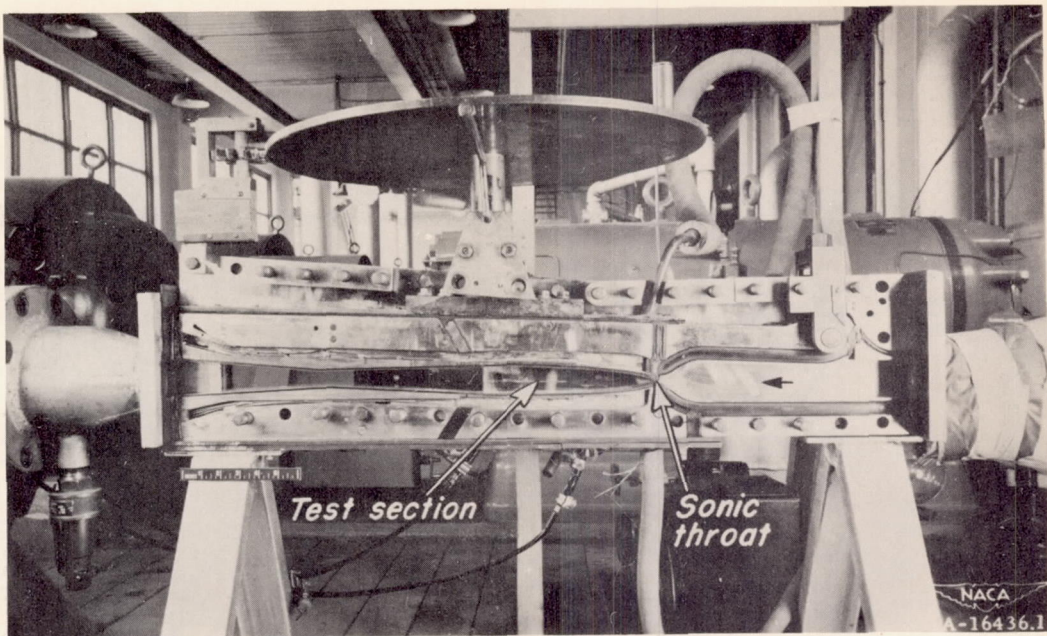
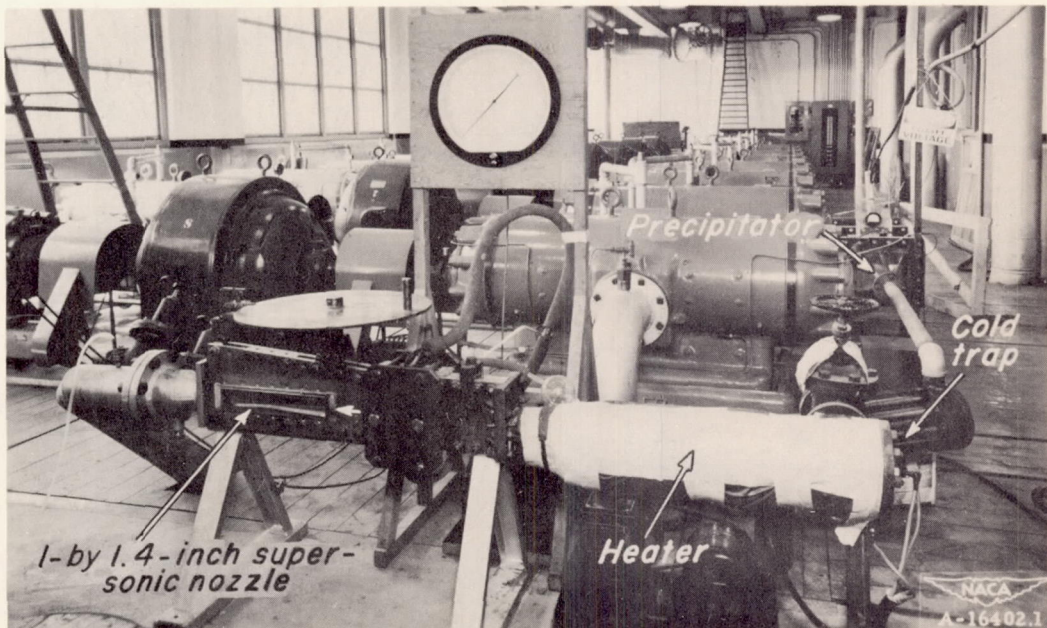


Figure 3.—Pressure-temperature diagram for the graphical determination of the effects of condensation of air in a supersonic air stream. $H_0 = 6$ atmospheres, $T_0 = 294^\circ \text{K}$.

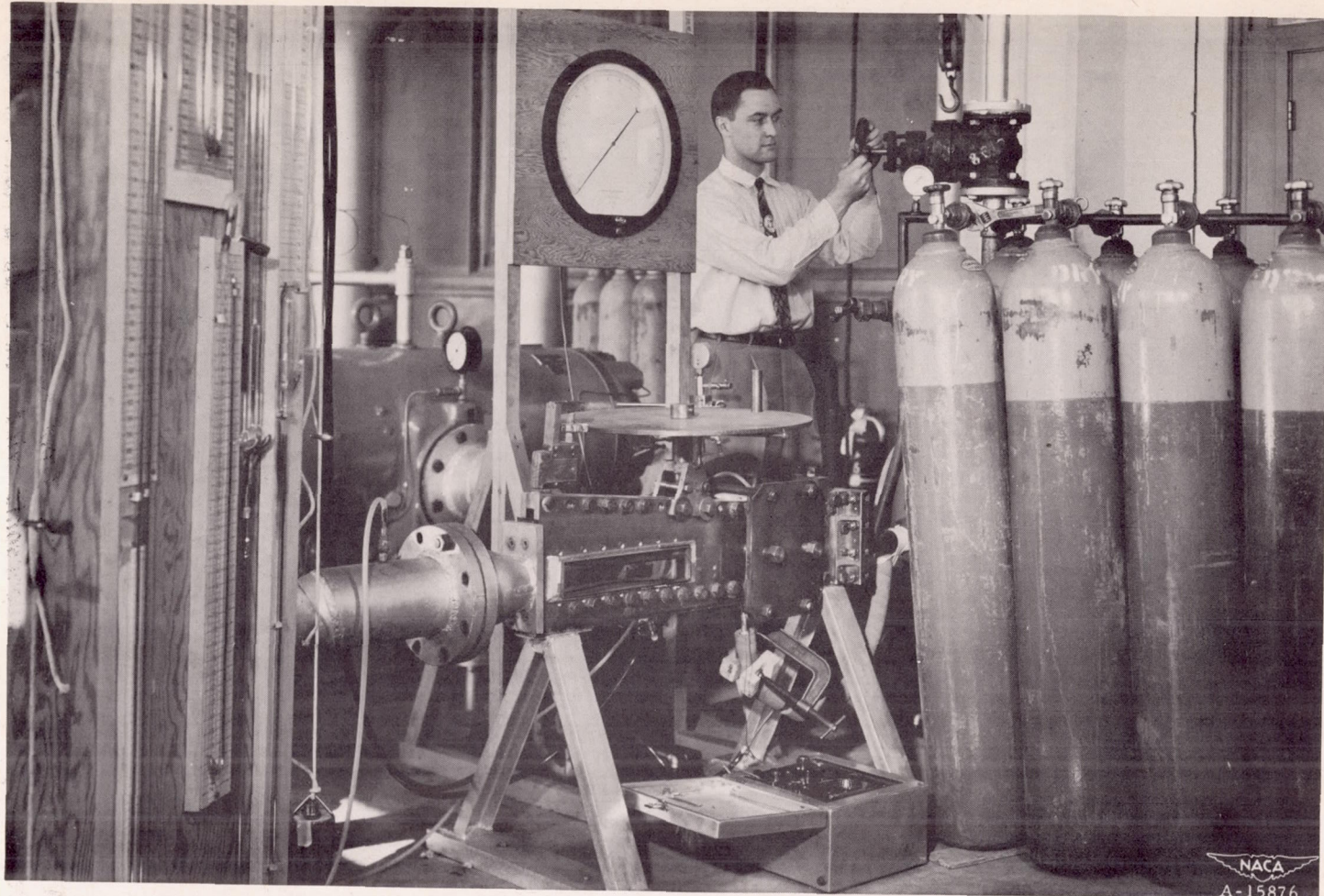


(a) View of nozzle with one sidewall removed.



(b) View of test setup showing air purification mechanisms and heater.

Figure 4.— The 1- by 1.4-inch supersonic nozzle.



(c) View of test setup showing compressed gas cylinders.

Figure 4.— Concluded.

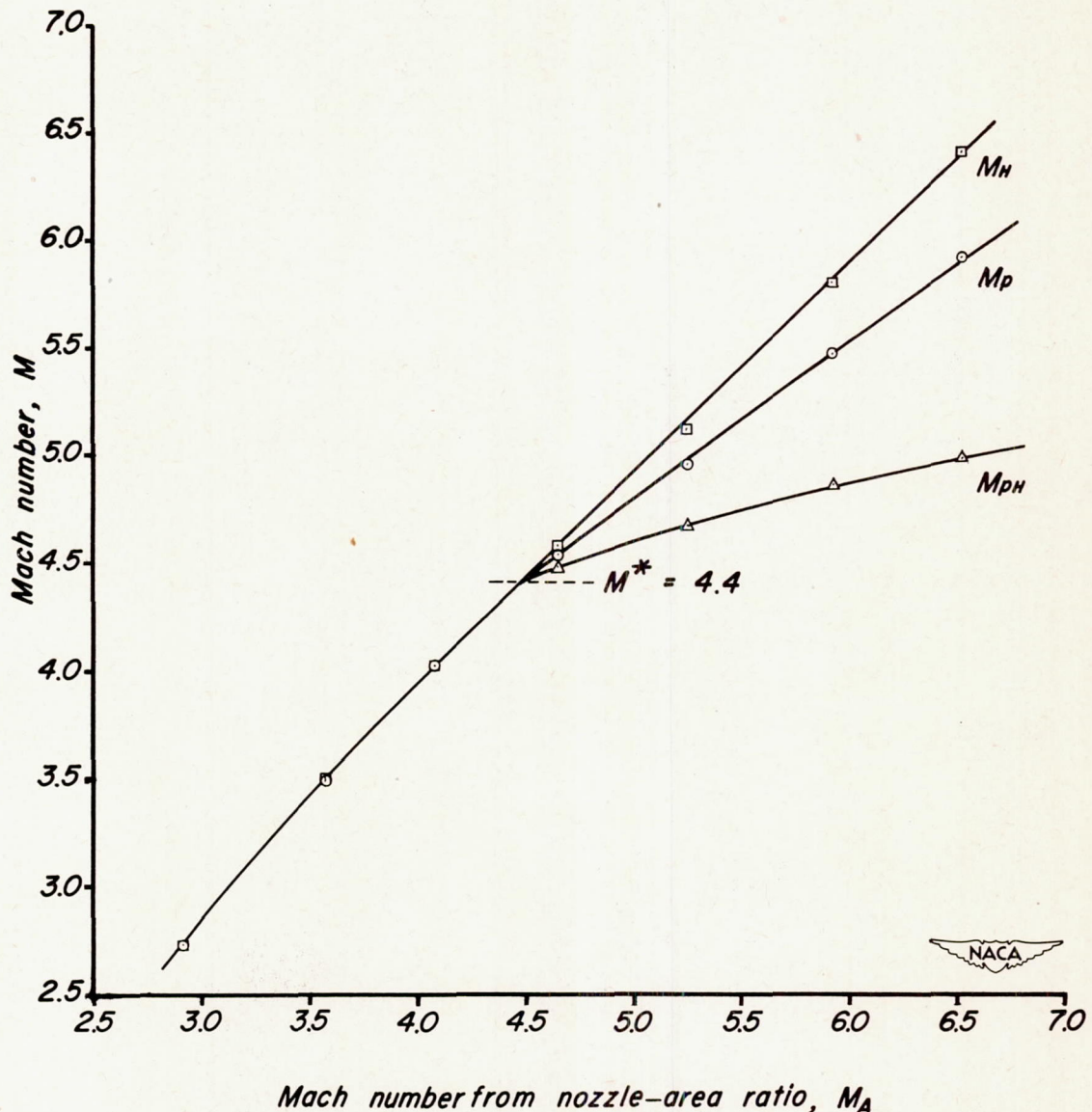


Figure 5.—Mach numbers as determined from various flow parameters in the Ames 10-by 14-inch supersonic wind tunnel as a function of Mach number from nozzle-area ratio. $H_0 = 6$ atmospheres, $T_0 = 288^\circ$ K.

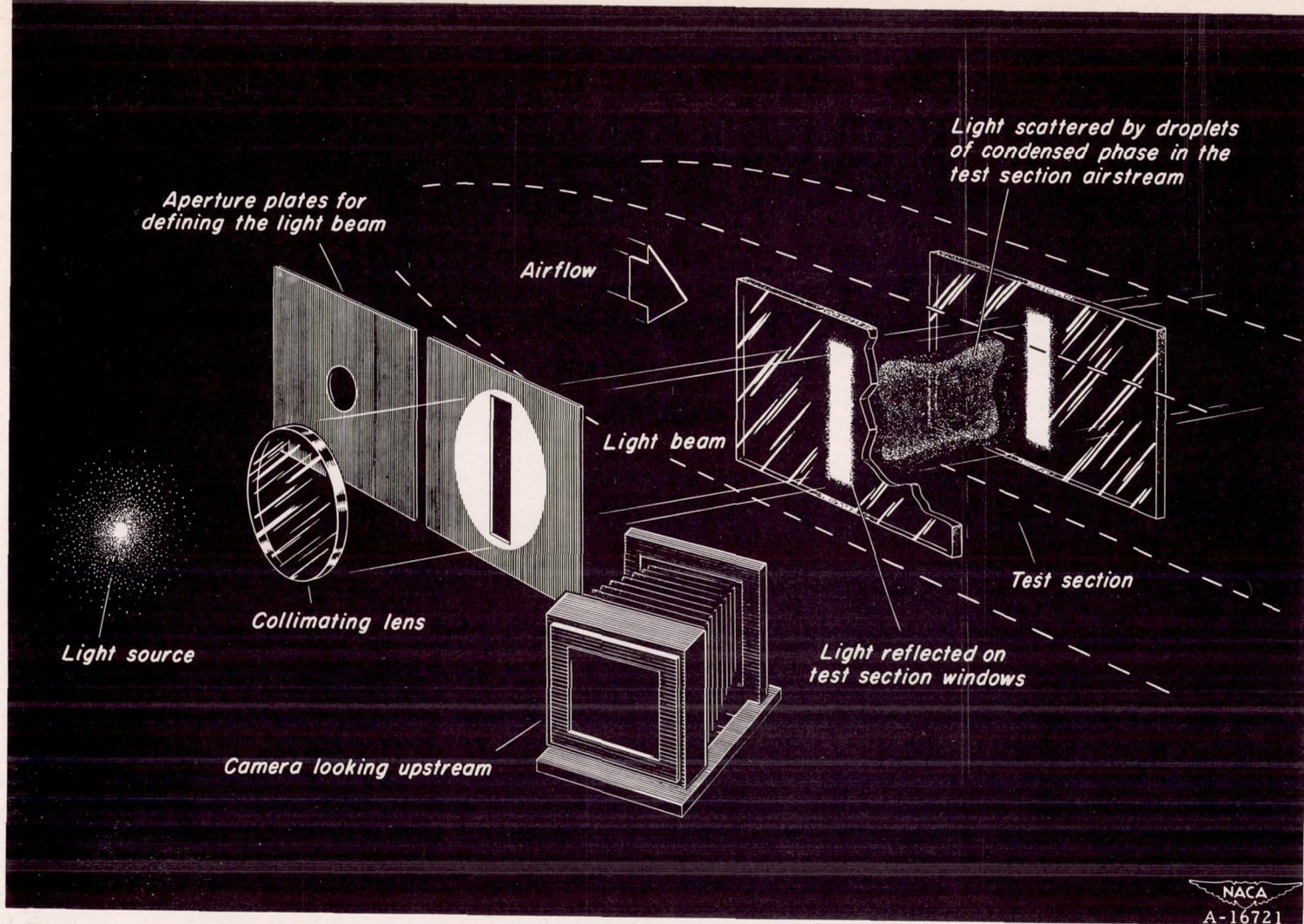
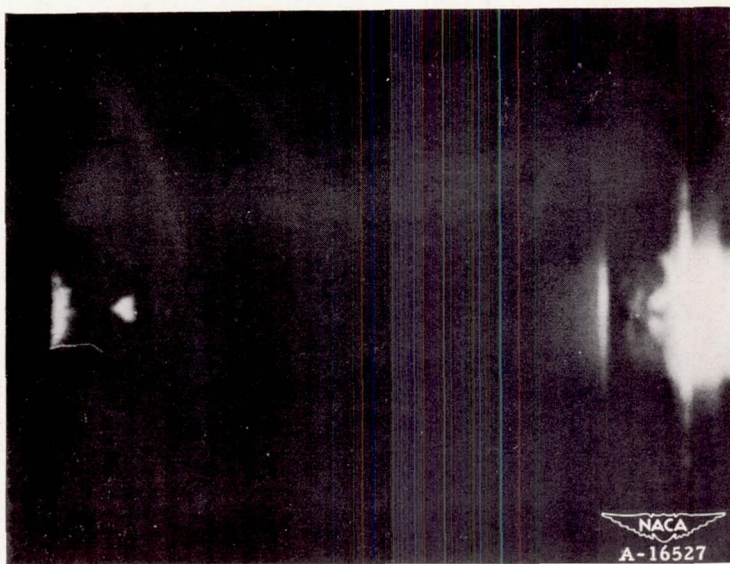
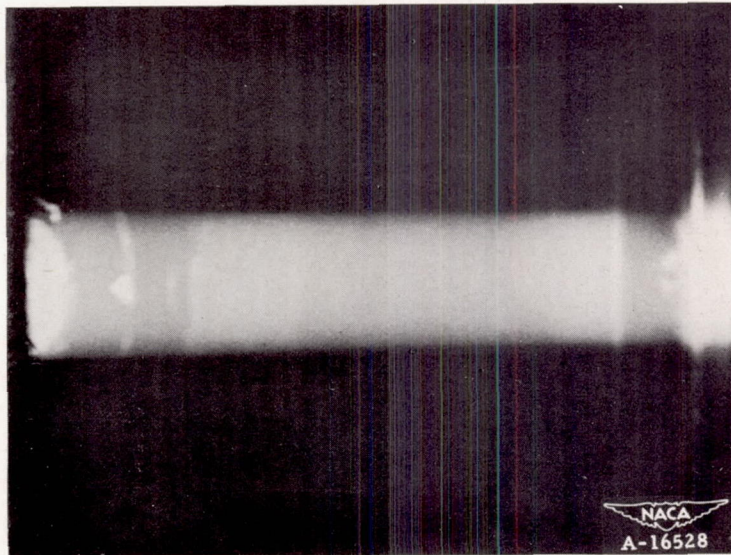


Figure 6.—Arrangement of apparatus used to photograph scattered light.

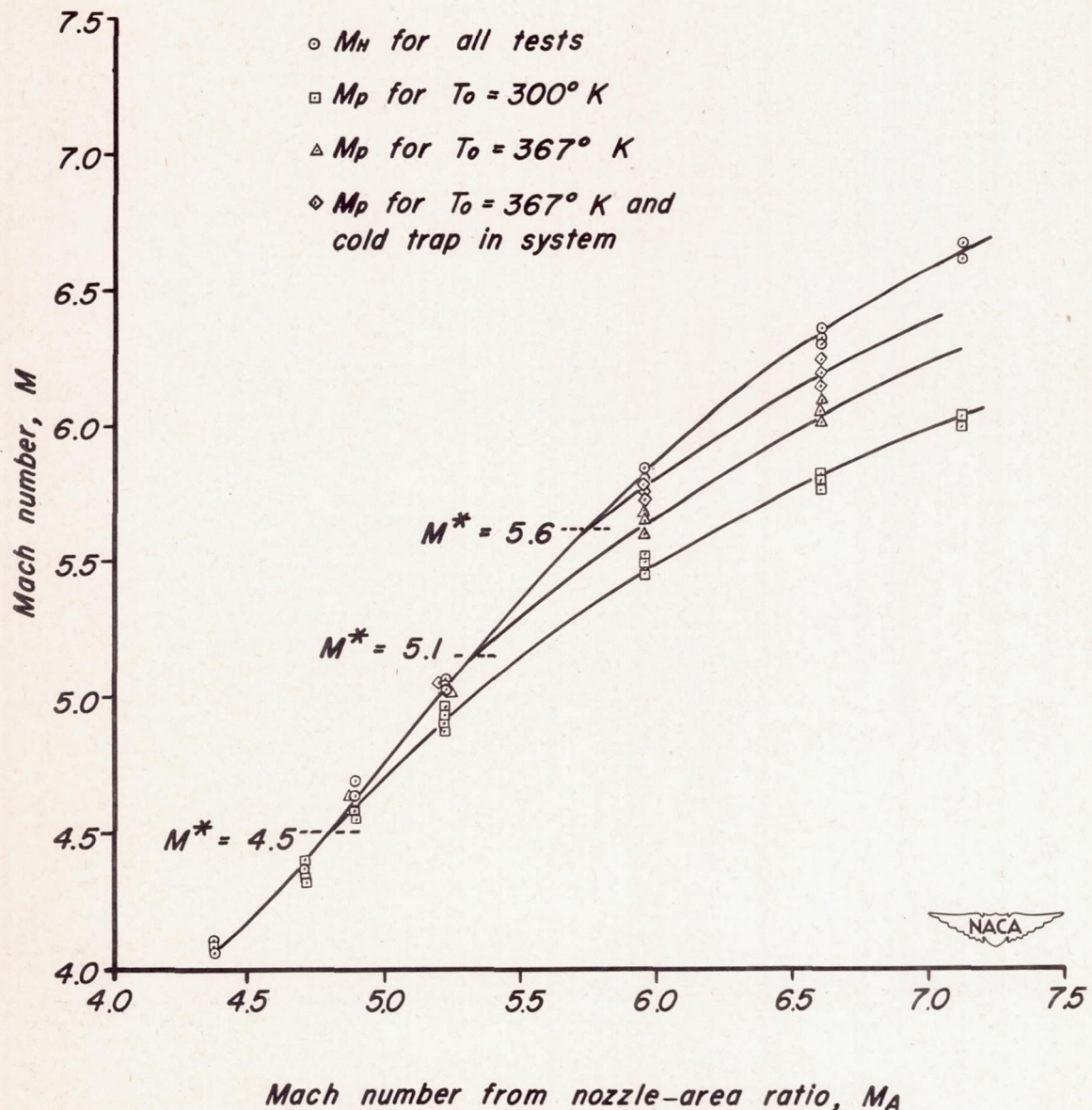


(a) Mach number less than threshold, $M_{pH} = 4.03$.



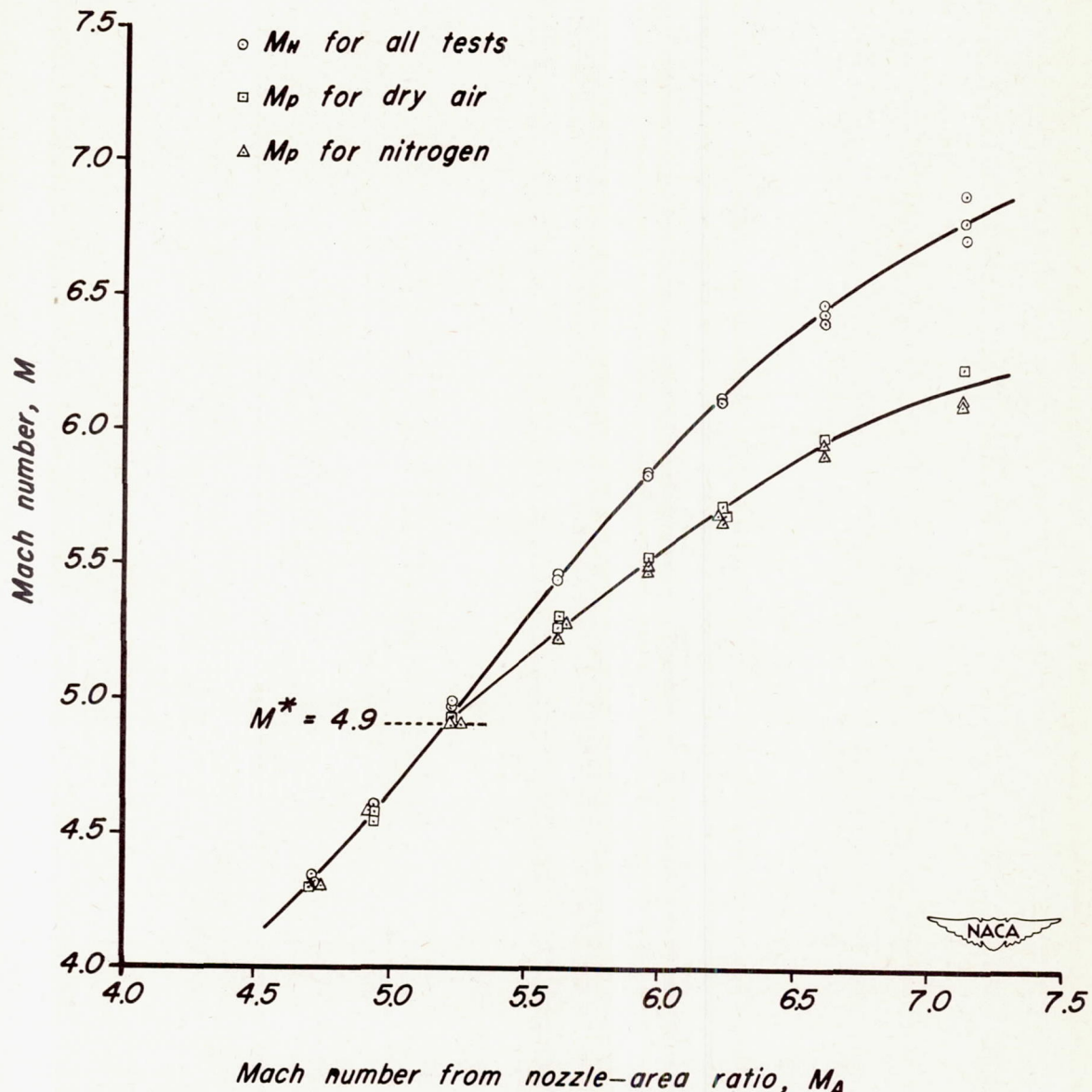
(b) Mach number greater than threshold, $M_{pH} = 4.67$.

Figure 7.— Light scattering from condensed air in the Ames 10- by 14-inch supersonic wind-tunnel air stream. $H_0 = 6$ atmospheres, $T_0 = 288^\circ\text{K}$, circular aperture.



(a) Normal supply air.

Figure 8.—Mach number in the 1-by 1.4-inch supersonic nozzle as a function of Mach number from nozzle-area ratio.
 $H_0 = 6$ atmospheres.



(b) Dry air and nitrogen. $T_0 = 278^\circ K.$

Figure 8.—Concluded.

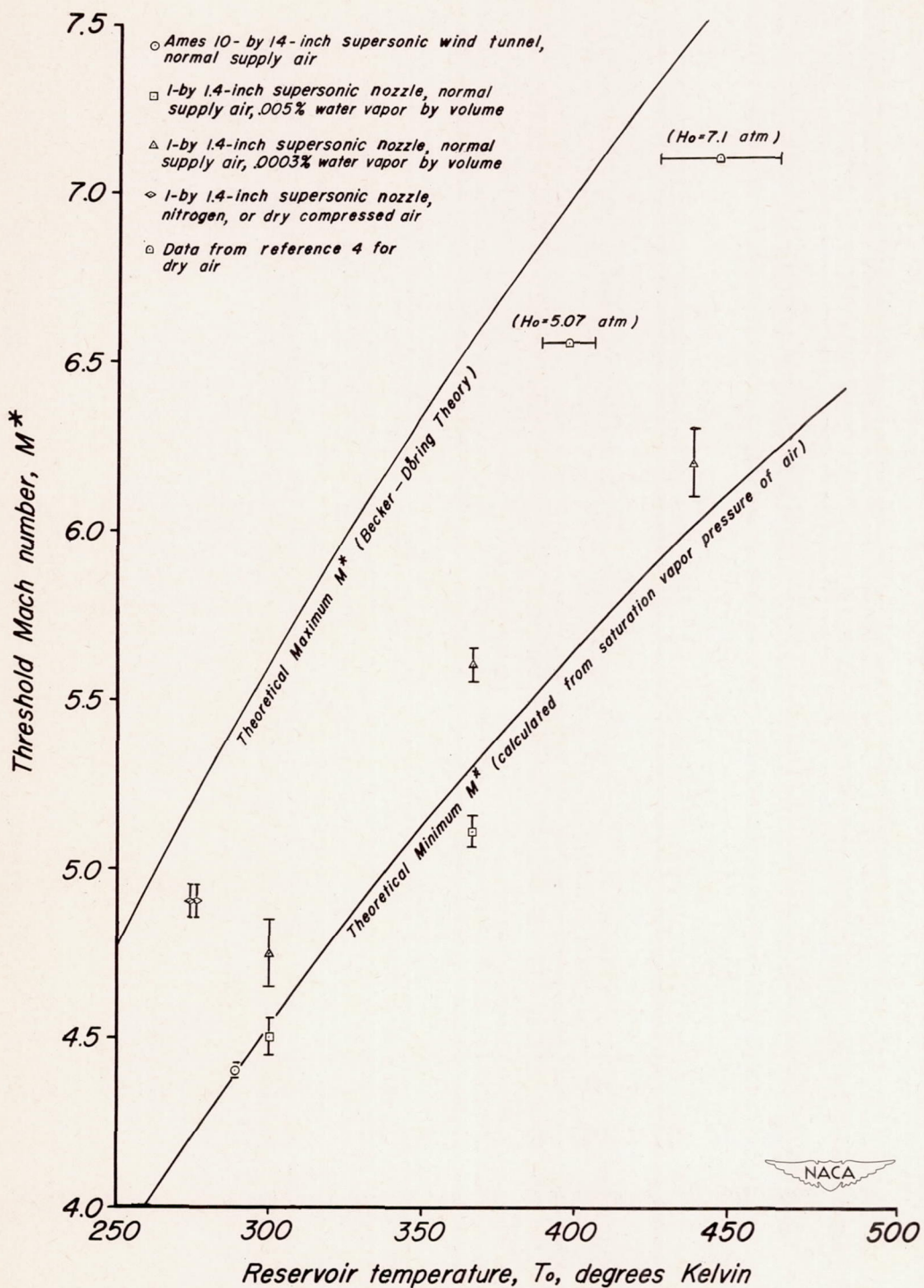
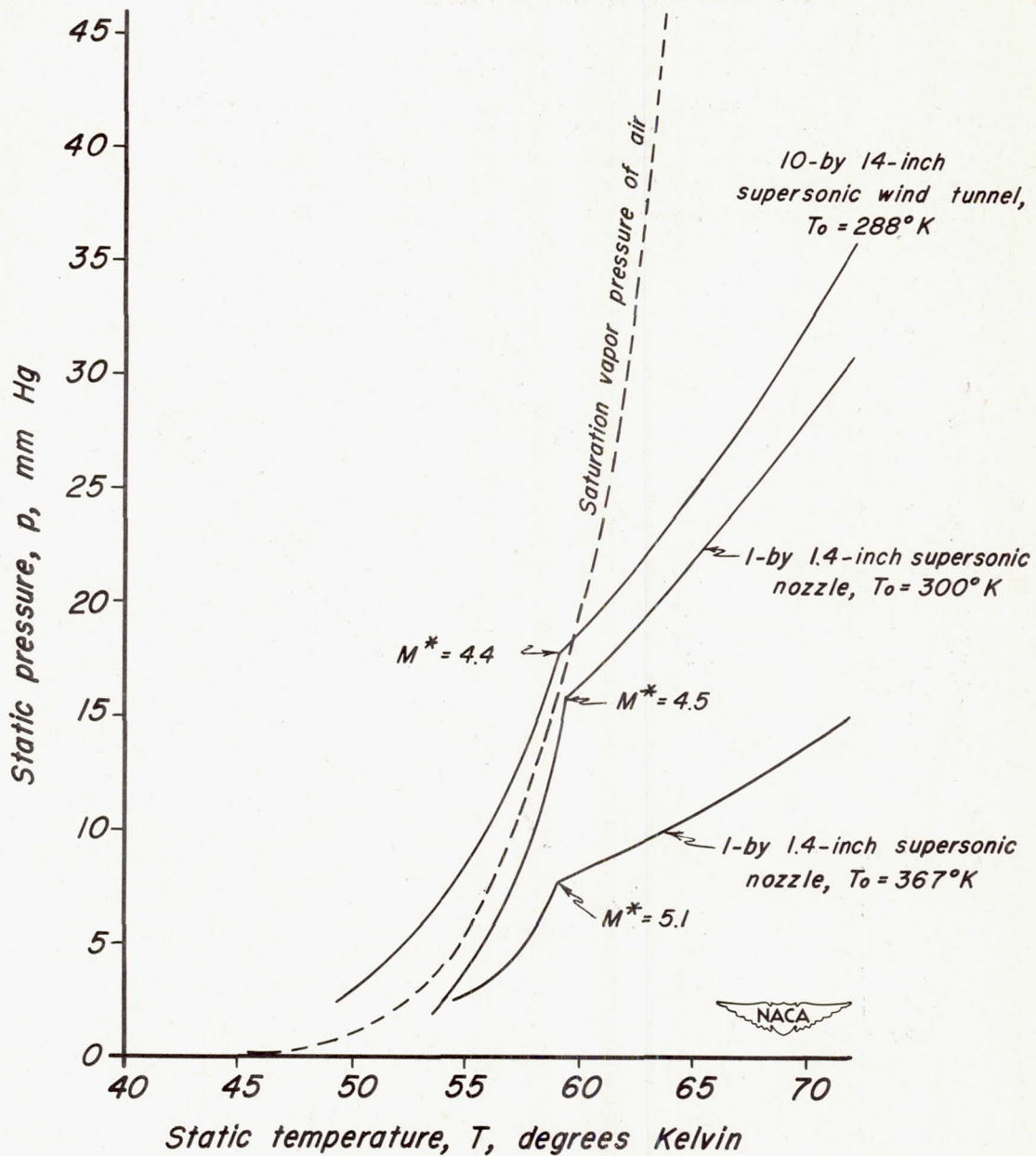
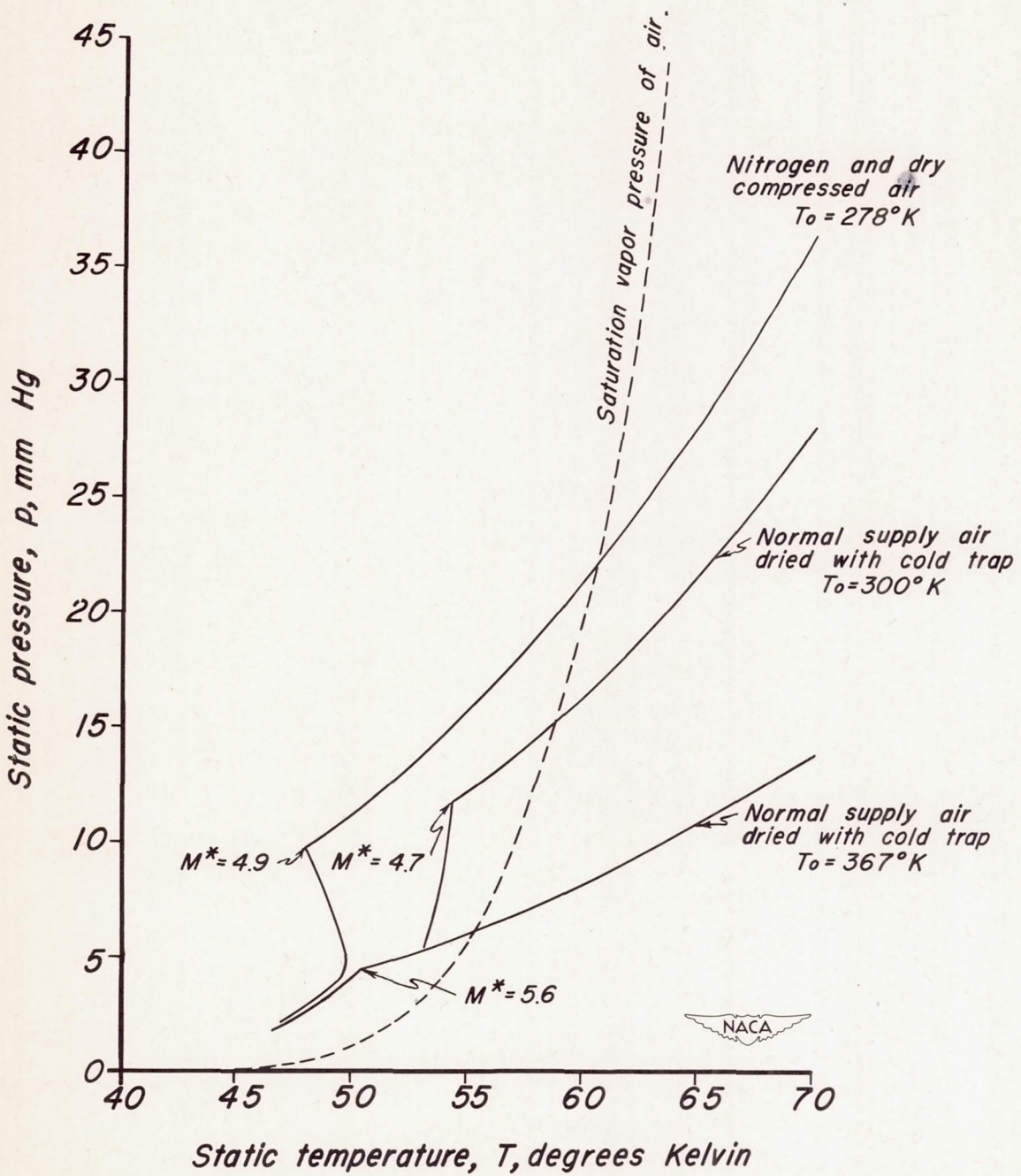


Figure 9.—Threshold Mach number, M^* , as a function of reservoir temperature, T_0 , ($H_0 = 6$ atmospheres except as noted).



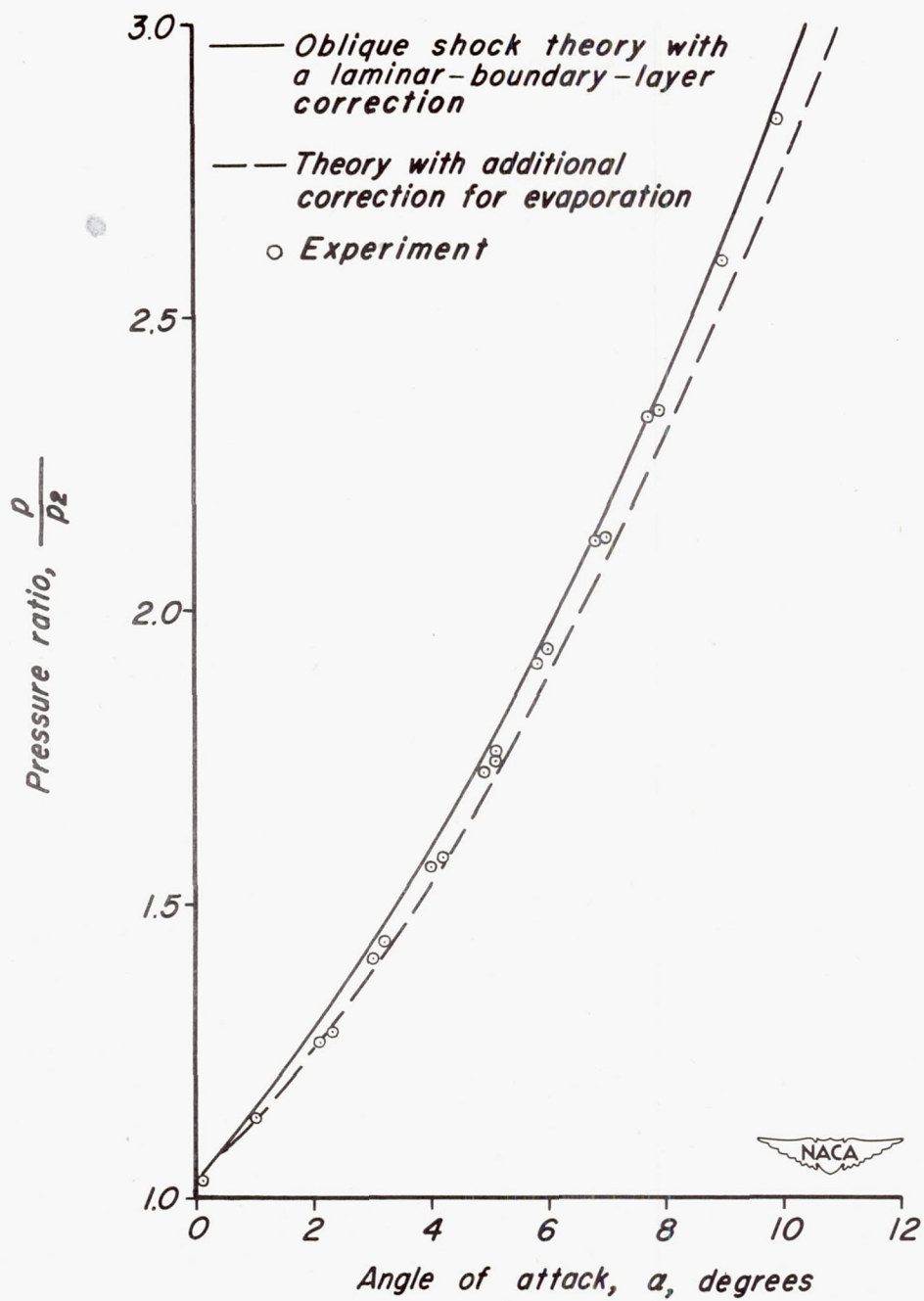
(a) Normal supply air expanded from various reservoir temperatures.

Figure 10.—Static pressure as a function of static temperature in supersonic wind tunnel flow. $H_0 = 6$ atmospheres.



(b) Purified gases expanded from various reservoir temperatures in the 1-by 1.4-inch supersonic nozzle.

Figure 10.—Concluded.



(a) $M_{\infty} = 4.48$

Figure 11.—Pressure ratio on a flat surface as a function of angle of attack.

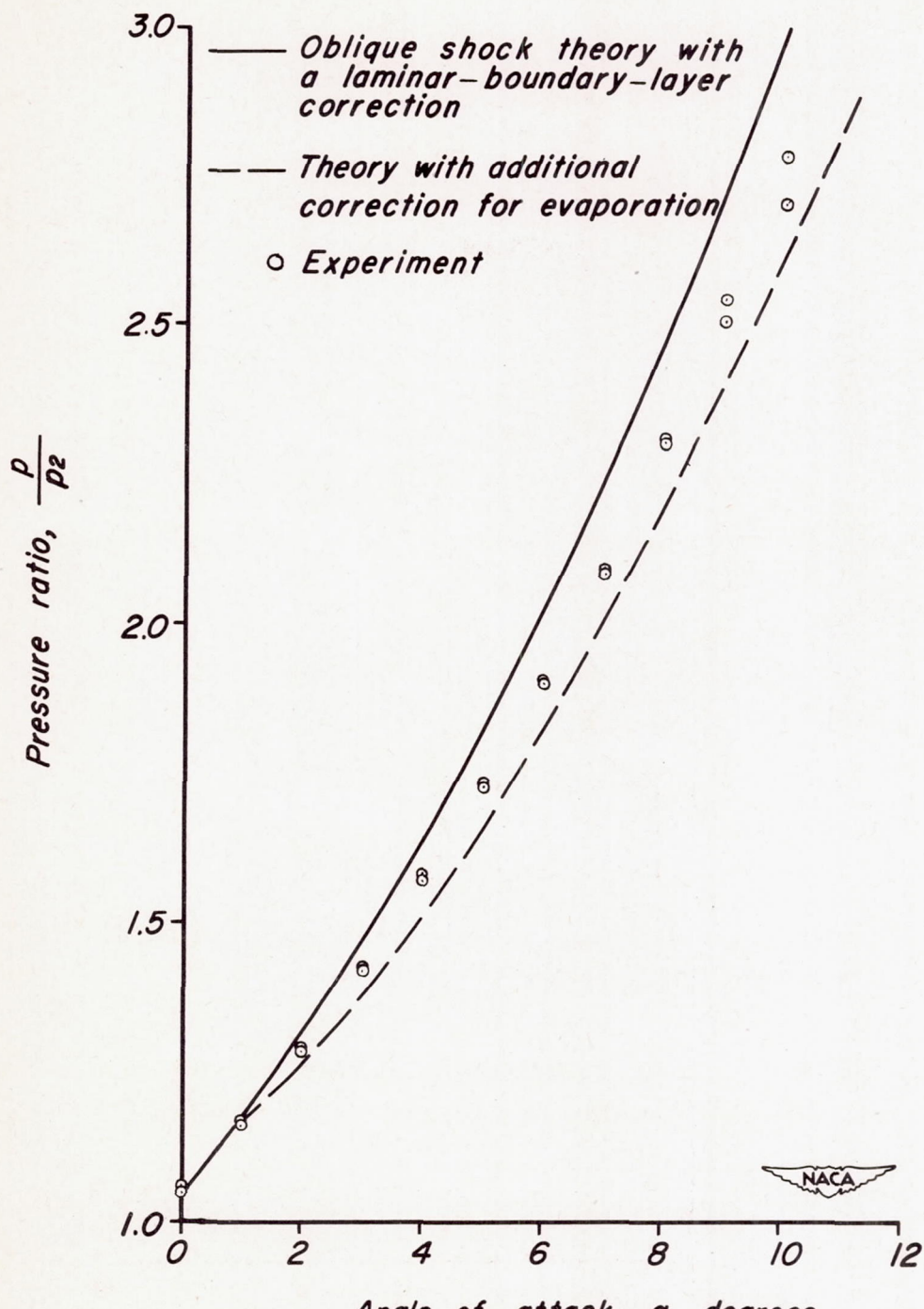
(b) $M_{ph} = 4.67$

Figure 11.—Continued.

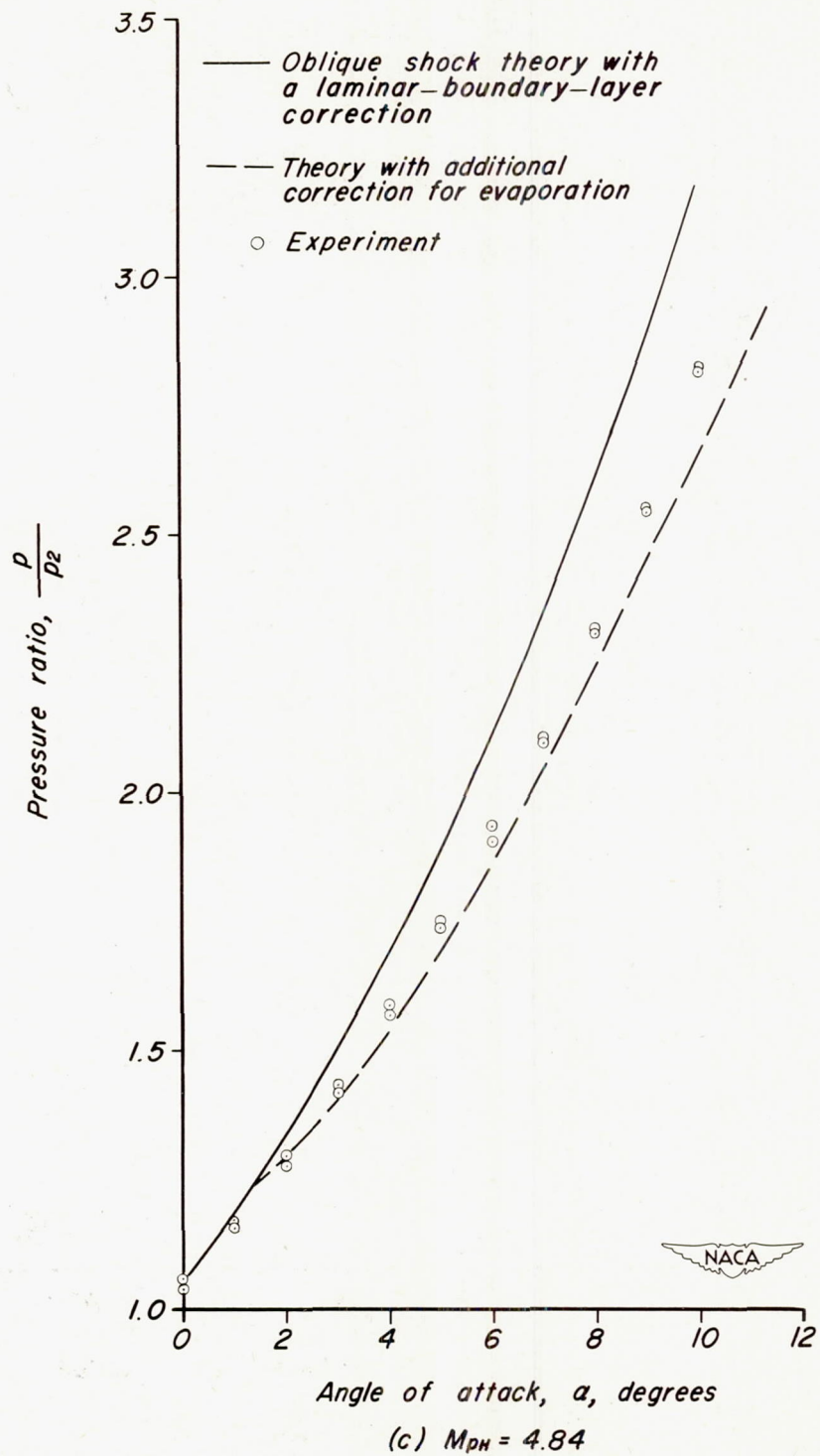


Figure 11.—Continued.

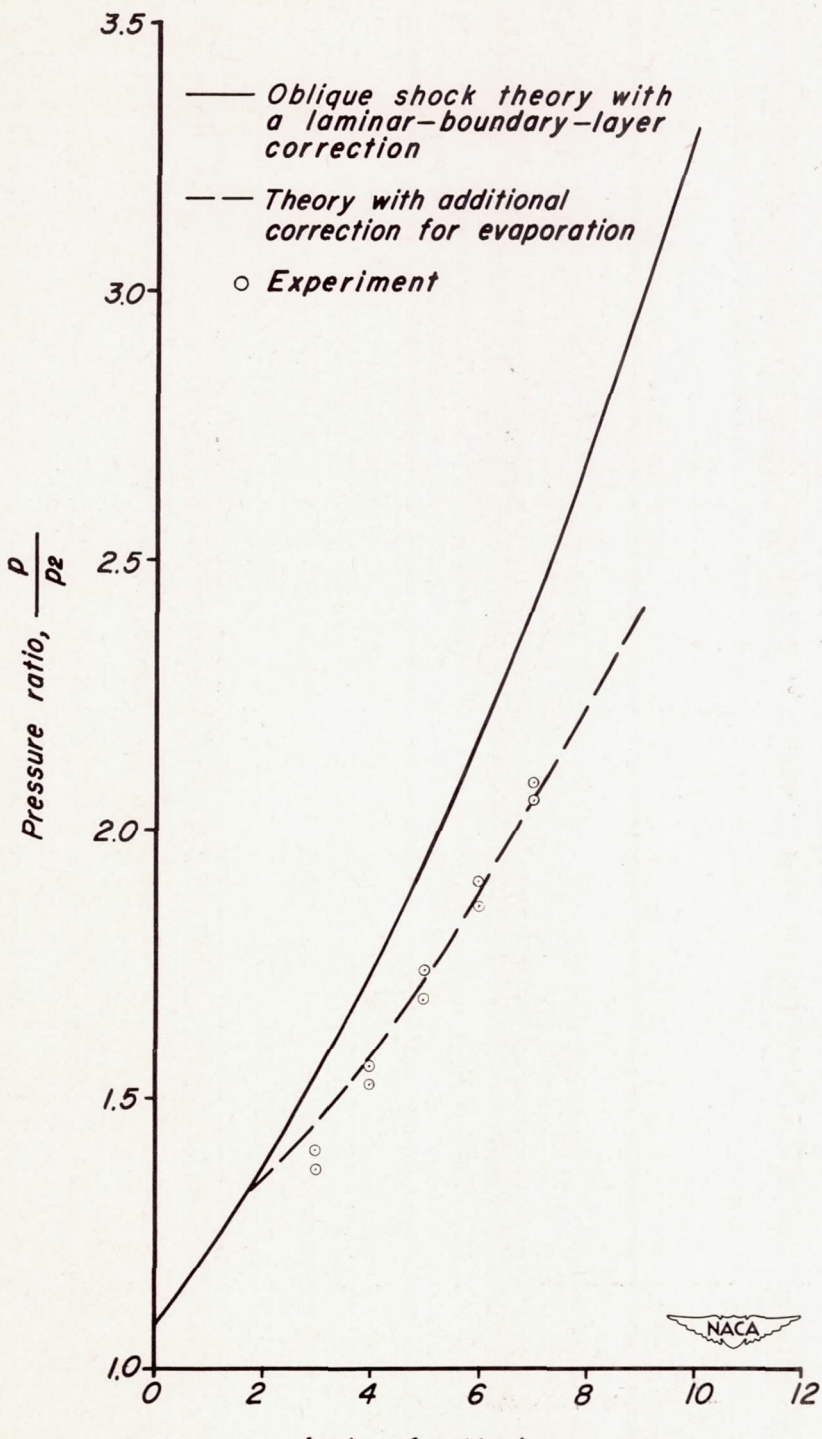
(d) $M_{\infty} = 4.98$

Figure 11.—Concluded.

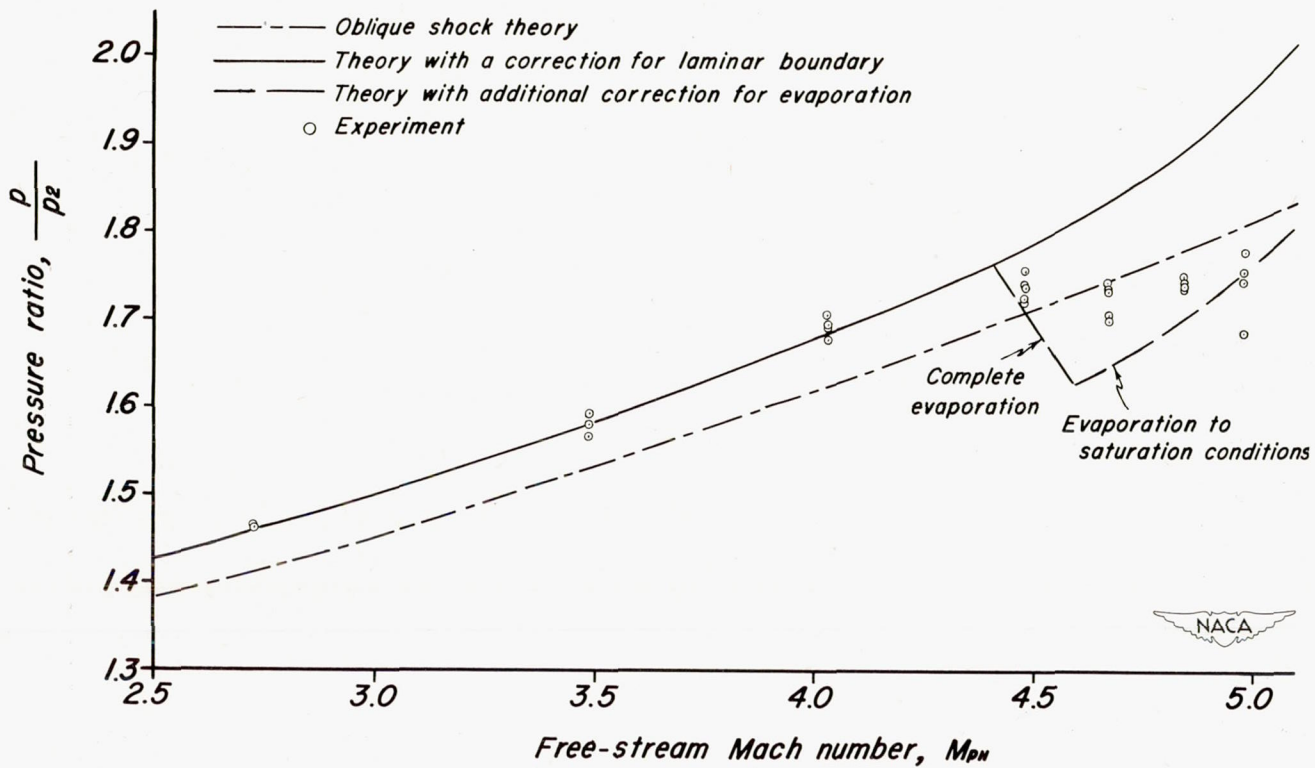
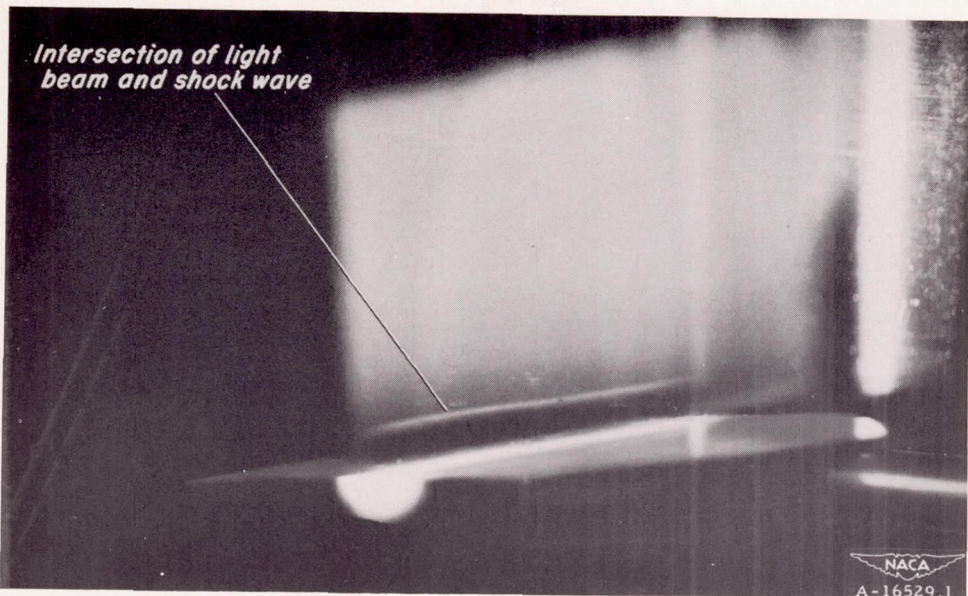
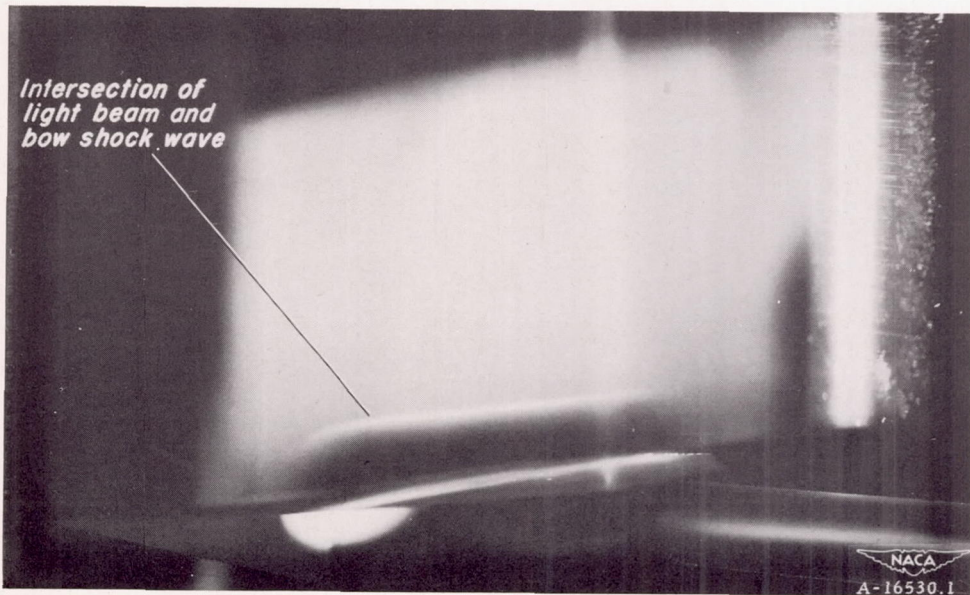


Figure 12.—Pressure ratio on a flat surface at 5° angle of attack as a function of Mach number.



(a) Light beam 1.5 inches from leading edge.



(b) Light beam 3 inches from leading edge.

Figure 13.— Light scattering about a flat surface at 5° angle of attack in the Ames 10- by 14-inch supersonic wind tunnel. $M_{pH} = 4.67$, $H_0 = 6$ atmospheres, $T_0 = 288^{\circ}\text{K}$, slit aperture.

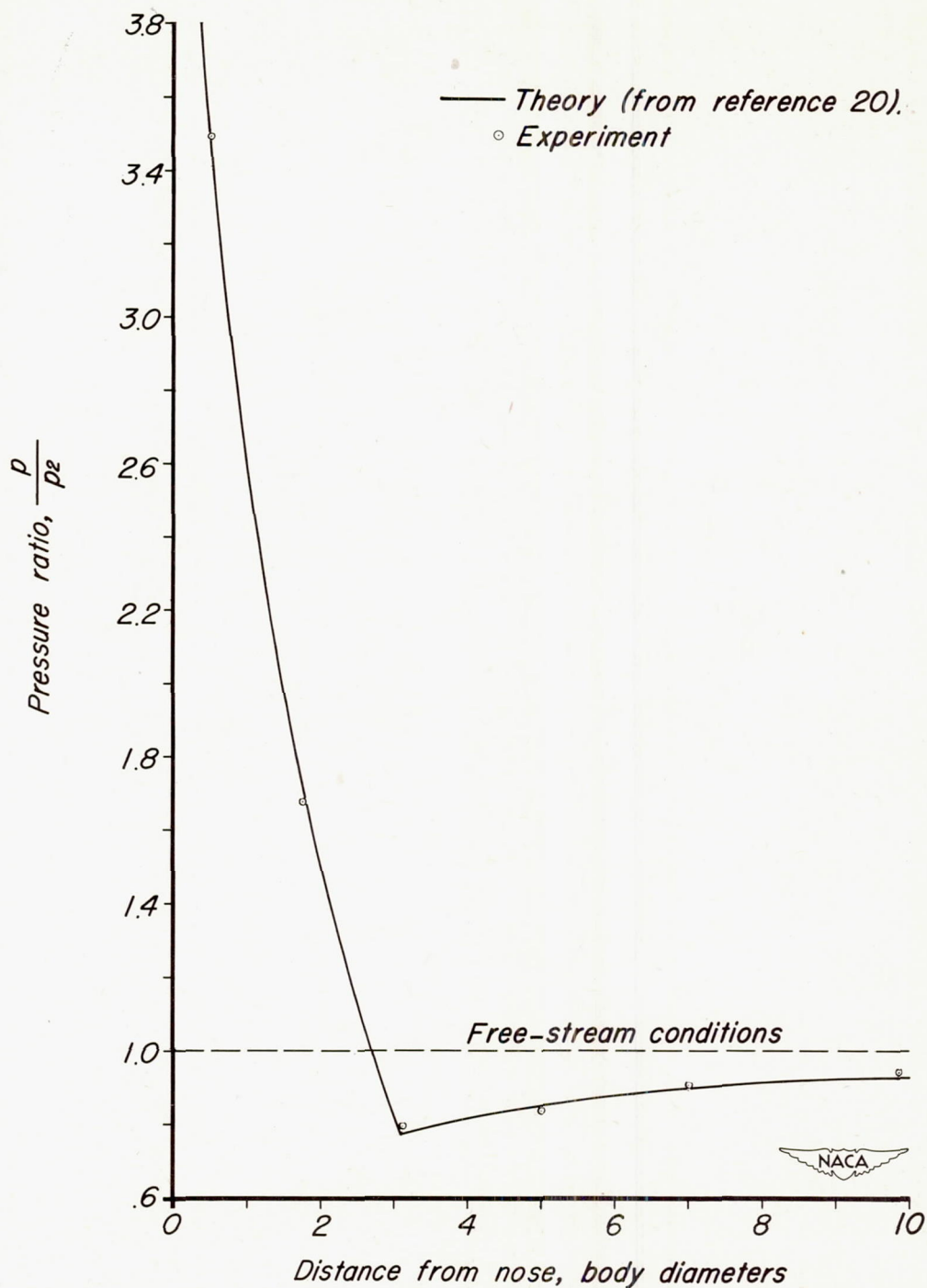
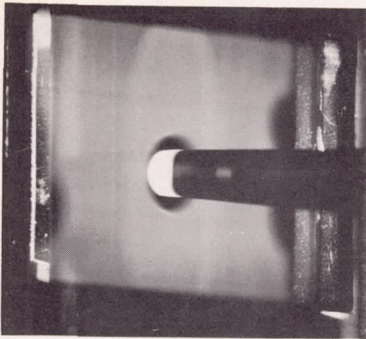
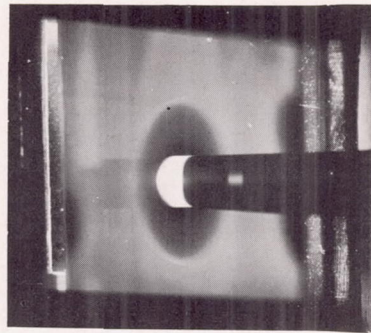


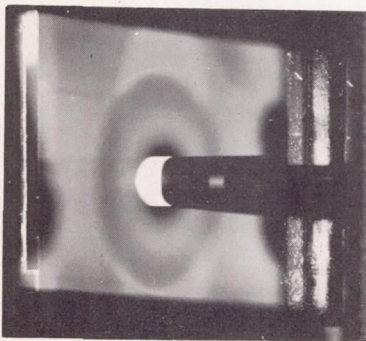
Figure 14.—Experimental and theoretical pressure distributions on a 10-caliber ogive-cylinder combination. $M_{\infty} = 4.67$.



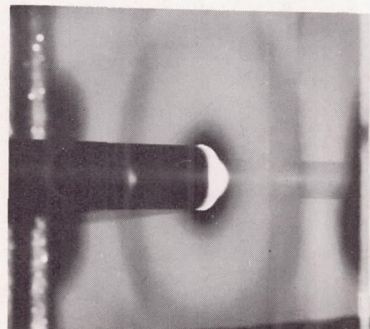
(a) Light beam 2.5 body diameters from nose, view looking upstream.



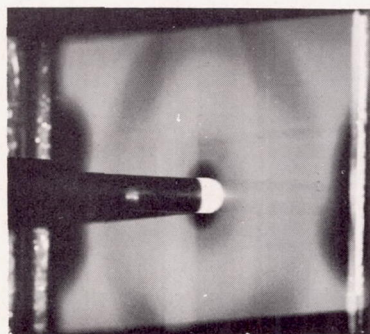
(b) Light beam 5.0 body diameters from nose, view looking upstream.



(c) Light beam 7.5 body diameters from nose, view looking upstream.



(d) Light beam 10 body diameters from nose, view looking downstream.



(e) Light beam 12.5 body diameters from nose, view looking downstream.

 A-16491

Figure 15.— Light scattering about a 10-caliber ogive-cylinder model in the Ames 10- by 14-inch supersonic wind tunnel. $M_{pH} = 4.67$, $H_0 = 6$ atmospheres, $T_0 = 288^{\circ}\text{K}$, slit aperture.